Acknowledgements. The dominant negative mutant of IκB was kindly provided by Dr Richard Gaynor (University of Texas Southwestern Medical Center at Dallas, Tex., USA). The authors are indebted to Naomasa Kakiya of the University of Tokyo for assistance in various areas of this study.

References

1. Betteridge DJ (2000) What is oxidative stress? Metabolism 49 [Suppl 1]:3–8
2. Reaven GM, Lithell H, Landsberg L (1996) Hypertension and associated metabolic abnormalities—the role of insulin resistance and the sympathoadrenal system. N Engl J Med 334:374–381
3. Tuck ML (1990) Metabolic considerations in hypertension. Am J Hypertens 3:355S–365S
4. Baynes JW (1991) Role of oxidative stress in development of complications in diabetes. Diabetes 40:405–412
5. Paolisso G, D'Amore A, Volpe C et al. (1994) Evidence for a relationship between oxidative stress and insulin action in non-insulin-dependent (type II) diabetic patients. Metabolism 43:1426–1429
6. Jones AF, Winkles JW, Jennings PE et al. (1988) Serum antioxidant activity in diabetes mellitus. Diabetes Res 7:89–92
7. Paolisso G, Di Maro G, Pizza G et al. (1992) Plasma GSH/GSSG affects glucose homeostasis in healthy subjects and non-insulin-dependent diabetics. Am J Physiol 263:E435–E440
8. Paolisso G, Balbi V, Volpe C et al. (1995) Metabolic benefits deriving from chronic vitamin C supplementation in aged non-insulin dependent diabetics. J Am Coll Nutr 14:387–392
9. Paolisso G, Di Maro G, Galzerano D et al. (1994) Pharmacological doses of vitamin E and insulin action in elderly subjects. Am J Clin Nutr 59:1291–1296
10. Rajagopalan S, Kurz S, Munzel T et al. (1996) Angiotensin II-mediated hypertension in the rat increases vascular superoxide production via membrane NADH/NADPH oxidase activation. Contribution to alterations of vasomotor tone. J Clin Invest 97:1916–1923
11. Schnackenberg CG, Wilcox CS (1999) Two-week administration of tempol attenuates both hypertension and renal excretion of 8-Iso prostaglandin f2alpha. Hypertension 33:424–428
12. Ogihara T, Asano T, Ando K et al. (2002) Angiotensin II-induced insulin resistance is associated with enhanced insulin signalling. Hypertension 40:872–879
13. Shimosawa T, Ogihara T, Matsui H et al. (2003) Deficiency of adrenomedullin induces insulin resistance by increasing oxidative stress. Hypertension 41:1080–1085
14. Meister A (1983) Selective modification of glutathione metabolism. Science 220:472–477
15. Khamaisi M, Kavel O, Rosenstock M et al. (2000) Effect of inhibition of glutathione synthesis on insulin action: in vivo and in vitro studies using buthionine sulfoximine. Biochem J 349:579–586
16. Vaziri ND, Wang XQ, Oveisi F, Rad B (2000) Induction of oxidative stress by glutathione depletion causes severe hypertension in normal rats. Hypertension 36:142–146
17. Ogihara T, Asano T, Ando K et al. (2001) Insulin resistance with enhanced insulin signalling in high-salt diet-fed rats. Diabetes 50:573–583
18. Yamamoto Y (1994) Chemiluminescence-based high-performance liquid chromatography assay of lipid hydroperoxides. Methods Enzymol 233:319–324
19. Anderson ME (1985) Determination of glutathione and glutathione disulfide in biological samples. Methods Enzymol 113:548–555
20. James DE, Burleigh KM, Kraegen EW (1986) In vivo glucose metabolism in individual tissues of the rat. Interaction between epinephrine and insulin. J Biol Chem 261:6366–6374
21. Hansen P, Gulve EA, Holloszy JO (1994) Suitability of 2-deoxyglucose for in vitro measurement of glucose transport activity in skeletal muscle. J Appl Physiol 76:979–985
22. Rodbell M (1964) Metabolism of isolated fat cells. I. Effects of hormones on glucose metabolism and lipolysis. J Biol Chem 239:375–380
23. Olefsky JM (1975) Effect of dexamethasone on insulin binding, glucose transport, and glucose oxidation of isolated rat adipocytes. J Clin Invest 56:1499–1508
24. Fujishiro M, Gotoh Y, Katagiri H et al. (2001) MKK6/3 and p38 MAPK pathway activation is not necessary for insulin-induced glucose uptake but regulates glucose transporter expression. J Biol Chem 276:19800–19806
25. Katagiri H, Asano T, Ishihara H et al. (1996) Overexpression of catalytic subunit p110alpha of phosphatidylinositol 3-kinase increases glucose transport activity with translocation of glucose transporters in 3T3-L1 adipocytes. J Biol Chem 271:16987–16990
26. Asano T, Kanda A, Katagiri H et al. (2000) p110beta is up-regulated during differentiation of 3T3-L1 cells and contributes to the highly insulin-responsive glucose transport activity. J Biol Chem 275:17671–17676
27. Satoh S, Nishimura H, Clark AE et al. (1993) Use of bismannose photolabel to elucidate insulin-regulated GLUT4 subcellular trafficking kinetics in rat adipose cells. Evidence that exocytosis is a critical site of hormone action. J Biol Chem 268:17820–17829
28. Anai M, Funaki M, Ogihara T et al. (1998) Altered expression levels and impaired steps in the pathway to phosphatidylinositol 3-kinase activation via insulin receptor substrates 1 and 2 in Zucker fatty rats. Diabetes 47:13–23
29. Sakoda H, Ogihara T, Anai M et al. (1999) No correlation of plasma cell 1 overexpression with insulin resistance in diabetic rats and 3T3-L1 adipocytes. Diabetes 48:1365–1371
30. Anai M, Ono H, Funaki M et al. (1998) Different subcellular distribution and regulation of expression of insulin receptor substrate (IRS)-3 from those of IRS-1 and IRS-2. J Biol Chem 273:29686–29692
31. Kriauciunas KM, Myers MG Jr, Kahn CR (2000) Cellular compartmentalization in insulin action: altered signaling by a lipid-modified IRS-1. Mol Cell Biol 20:6849–6859
32. Lu B, Ennis D, Lai R et al. (2001) Enhanced sensitivity of insulin-resistant adipocytes to vanadate is associated with oxidative stress and decreased reduction of vanadate (+5) to vanadyl (+4). J Biol Chem 276:35589–35598
33. Schreck R, Albermann K, Baeuerle PA (1992) Nuclear factor kappa B: an oxidative stress-responsive transcription factor of eukaryotic cells (a review). Free Radic Res Commun 17:221–237
34. Siebenlist U, Franzoso G, Brown K (1994) Structure, regulation and function of NF-kappa B. Annu Rev Cell Biol 10:405–455
35. Leeuwenburgh C, Ji LL (1995) Glutathione depletion in rested and exercised mice: biochemical consequence and adaptation. Arch Biochem Biophys 316:941–949
36. Czech MP (1995) Molecular actions of insulin on glucose transport. Annu Rev Nutr 15:441–471

37. Saad MJ, Folli F, Kahn JA, Kahn CR (1993) Modulation of insulin receptor, insulin receptor substrate-1, and phosphatidylinositol 3-kinase in liver and muscle of dexamethasone-treated rats. J Clin Invest 92:2065–2072
38. Cusi K, Maezono K, Osman A et al. (2000) Insulin resistance differentially affects the PI 3-kinase- and MAP kinase-mediated signalling in human muscle. J Clin Invest 105:311–320
39. Rudich A, Tirosh A, Potashnik R, Hemi R, Kanety H, Bashan N (1998) Prolonged oxidative stress impairs insulin-induced GLUT4 translocation in 3T3-L1 adipocytes. Diabetes 47:1562–1569
40. Tirosh A, Potashnik R, Bashan N, Rudich A (1999) Oxidative stress disrupts insulin-induced cellular redistribution of insulin receptor substrate-1 and phosphatidylinositol 3-kinase in 3T3-L1 adipocytes. A putative cellular mechanism for impaired protein kinase B activation and GLUT4 translocation. J Biol Chem 274:10595–10602
41. Schreck R, Rieber P, Baeuerle PA (1991) Reactive oxygen intermediates as apparently widely used messengers in the activation of the NF-kappa B transcription factor and HIV-1. EMBO J 10:2247–2258
42. Suzuki YJ, Packer L (1993) Inhibition of NF-kappa B activation by vitamin E derivatives. Biochem Biophys Res Commun 193:277–283
43. Sen CK, Packer L (1996) Antioxidant and redox regulation of gene transcription. FASEB J 10:709–720
44. Yamamoto Y, Gaynor RB (2001) Therapeutic potential of inhibition of the NF-kappaB pathway in the treatment of inflammation and cancer. J Clin Invest 107:135–142
45. Baeuerle PA, Henkel T (1994) Function and activation of NF-kappa B in the immune system. Annu Rev Immunol 12:141–179
46. Barnes PJ, Karin M (1997) Nuclear factor-kappaB: a pivotal transcription factor in chronic inflammatory diseases. N Engl J Med 336:1066–1071
47. Sizemore N, Leung S, Stark GR (1999) Activation of phosphatidylinositol 3-kinase in response to interleukin-1 leads to phosphorylation and activation of the NF-kappaB p65/RelA subunit. Mol Cell Biol 19:4798–4805
48. Reddy SA, Huang JH, Liao WS (2000) Phosphatidylinositol 3-kinase as a mediator of TNF-induced NF-kappa B activation. J Immunol 164:1355–1363
49. Kim JK, Kim YJ, Fillmore JJ et al. (2001) Prevention of fat-induced insulin resistance by salicylate. J Clin Invest 108:437–446
50. Yuan M, Konstantopoulos N, Lee J et al. (2001) Reversal of obesity- and diet-induced insulin resistance with salicylates or targeted disruption of Ikkbeta. Science 293:1673–1677

ELSEVIER

Available online at www.sciencedirect.com
SCIENCE DIRECT®

Biochemical and Biophysical Research Communications 322 (2004) 310–319

BBRC

www.elsevier.com/locate/ybbrc

Atrial natriuretic peptide inhibits cardiomyocyte hypertrophy through mitogen-activated protein kinase phosphatase-1

Doubun Hayashi[a,b], Sumiyo Kudoh[a], Ichiro Shiojima[a], Yunzeng Zou[d], Koichiro Harada[a], Masaki Shimoyama[a], Yasushi Imai[a], Koshiro Monzen[a,b], Tsutomu Yamazaki[a,c], Yoshio Yazaki[e], Ryozo Nagai[a], Issei Komuro[d,*]

[a] *Department of Cardiovascular Medicine, University of Tokyo Graduate School of Medicine, 7-3-1 Hongo, Bunkyo-ku, Tokyo 113-8655, Japan*
[b] *Department of Pharmacoepidemiology, University of Tokyo Graduate School of Medicine, 7-3-1 Hongo, Bunkyo-ku, Tokyo 113-8655, Japan*
[c] *Department of Clinical Bioinformatics, University of Tokyo Graduate School of Medicine, 7-3-1 Hongo, Bunkyo-ku, Tokyo 113-8655, Japan*
[d] *Department of Cardiovascular Science and Medicine, Chiba University Graduate School of Medicine, 1-8-1 Inohana, Chuo-ku, Chiba 260-8670, Japan*
[e] *International Medical Center of Japan, 1-21-1 Toyama, Shinjuku-ku, Tokyo 162-8655, Japan*

Received 5 June 2004

Abstract

Cardiac hypertrophy is formed in response to hemodynamic overload. Although a variety of factors such as catecholamines, angiotensin II (AngII), and endothelin-1 (ET-1) have been reported to induce cardiac hypertrophy, little is known regarding the factors that inhibit the development of cardiac hypertrophy. Production of atrial natriuretic peptide (ANP) is increased in the hypertrophied heart and ANP has recently been reported to inhibit the growth of various cell types. We therefore examined whether ANP inhibits the development of cardiac hypertrophy. Pretreatment of cultured cardiomyocytes with ANP inhibited the AngII- or ET-1-induced increase in the cell size and the protein synthesis. ANP also inhibited the AngII- or ET-1-induced hypertrophic responses such as activation of mitogen-activated protein kinase (MAPK) and induction of immediate early response genes and fetal type genes. To determine how ANP inhibits cardiomyocyte hypertrophy, we examined the mechanism of ANP-induced suppression of the MAPK activation. ANP strongly induced expression of MAPK phosphatase-1 (MKP-1) and overexpression of *MKP-1* inhibited AngII- or ET-1-induced hypertrophic responses. These growth-inhibitory actions of ANP were mimicked by a cyclic GMP analog 8-bromo-cyclic GMP. Taken together, ANP directly inhibits the growth factor-induced cardiomyocyte hypertrophy at least partly via induction of MKP-1. Our present study suggests that the formation of cardiac hypertrophy is regulated not only by positive but by negative factors in response to hemodynamic load.
© 2004 Elsevier Inc. All rights reserved.

Keywords: Angiotensin II; Atrial natriuretic peptide; Cardiac hypertrophy; Cardiomyocyte; Cyclic GMP; Endothelin-1; Growth factor; MAPK phosphatase-1; Mitogen-activated protein kinase; Vasoactive peptide

Since cardiac myocytes virtually lose their proliferative ability soon after birth, they respond to external stimuli not by increasing the cell number but by increasing the individual cell volume, called hypertrophy. Although cardiac hypertrophy has been considered to be a beneficial adaptive response of the heart to the increased workload, the hypertrophic heart often leads to dilated cardiomyopathy and eventually causes congestive heart failure after sustained overload [1]. Recent clinical studies have demonstrated that the increased ventricular mass is an independent risk factor for cardiac morbidity and mortality [2]. Therefore, it has become even more important to elucidate the molecular mechanism of how cardiac hypertrophy is formed.

* Corresponding author. Fax: +81 43 226 2557.
E-mail address: komuro-tky@umin.ac.jp (I. Komuro).

0006-291X/$ - see front matter © 2004 Elsevier Inc. All rights reserved.
doi:10.1016/j.bbrc.2004.07.119

A variety of factors have been implicated in the pathogenesis of cardiac hypertrophy [3]. Vasoactive peptides such as angiotensin II (AngII) [3–7] and endothelin-1 (ET-1) [8,9] have been reported to induce cardiomyocyte hypertrophy by autocrine or paracrine mechanisms. These factors are produced and secreted in the heart in response to the increased overload and induce cardiomyocyte hypertrophy. Antagonists of these factors effectively inhibit the load-induced cardiomyocyte hypertrophy [6–9]. The intracellular signaling pathways initiated by these growth factors and the resultant hypertrophic responses in cardiomyocytes have also been intensively investigated. AngII and ET-1 activate various protein kinases including protein kinase C and the mitogen-activated protein kinase (MAPK) family. Activation of these protein kinases induces expression of many specific genes [10–12] and an increase in protein synthesis [12].

Among the genes that are upregulated in the hypertrophied heart, atrial natriuretic peptide (ANP) has unique features. ANP reduces the hemodynamic load as a potent vasorelaxing and diuretic–natriuretic peptide, which indirectly inhibits the development of cardiac hypertrophy [13]. In addition to the indirect effects of ANP via hemodynamics, ANP has recently been reported to have direct growth-inhibitory effects in various cell types such as vascular smooth muscle cells, glomerular mesangial cells, endothelial cells, cardiac fibroblasts, and astrocytes [14–19]. In these cells, 8-bromo-cyclic GMP (8-Br-cGMP), a cell permeable analog of cyclic GMP (cGMP), mimicked the effects of ANP, indicating that the growth-inhibitory effects of ANP are dependent on cGMP. Furthermore, it has recently been reported that ANP induces expression of MAPK phosphatase-1 (MKP-1) [20]. MKP-1 is a dual serine/threonine and tyrosine phosphatase and specifically inactivates MAPK family members [21]. Overexpression of MKP-1 blocks the MAPK-dependent gene expression and inhibits cell proliferation [22–24]. These observations suggest that ANP may exert its inhibitory effects on cell growth through inactivation of MAPK family members by induction of MKP-1. Three members of the MAPK family, the extracellular signal-regulated kinases (ERKs), the c-Jun NH_2-terminal kinases/stress-activated protein kinases (JNKs/SAPKs), and p38MAPKs, have been shown to be activated by hypertrophic stimuli in cardiac myocytes and have been implicated in the development of cardiac hypertrophy [25–30].

In the present study, we examined whether ANP has direct inhibitory effects on growth factor-induced cardiomyocyte hypertrophy. Pretreatment with ANP suppressed the growth factor-induced increase in the cell volume and the protein synthesis of cardiomyocytes. ANP also inhibited hypertrophic responses such as activation of MAPK and induction of immediate early response genes and fetal type genes. In addition, ANP strongly induced expression of MKP-1 in cardiac myocytes and overexpression of *MKP-1* suppressed AngII-induced gene expressions. These results suggest that anti-hypertrophic effects of ANP are, at least in part, mediated by inactivation of MAPK via induction of MKP-1. These inhibitory actions of ANP were mimicked by a cGMP analog, 8-Br-cGMP.

Materials and methods

Reagents. [γ-^{32}P]ATP and [^{3}H]phenylalanine were purchased from Du Point-New England Nuclear. Dulbecco's modified Eagle's medium (DMEM) and fetal bovine serum (FBS) were from Gibco-BRL. Polyclonal antibodies against MKP-1 were purchased from Santa Cruz Biotechnology. A rat ANP [1–28], AngII, myelin basic protein (MBP), and other reagents were purchased from Sigma.

Cell culture. Primary cultures of cardiomyocytes were prepared from ventricles of 1-day-old Wistar rats as described previously [6]. Except for the reporter gene assay, cells were plated at a field density of 1×10^3 cells/mm^2 on 35-mm culture dishes and cultured in DMEM with 10% FBS for the first 24h, and then the culture medium was changed to DMEM containing 0.1% FBS. After 48h of serum starvation, cardiomyocytes were stimulated by various agents. For transfection and reporter gene assay, cells were plated at the same density, and subjected to transfection after 24h of culture in DMEM with 10% FBS.

Immunofluorescence. Immunostaining of cardiomyocytes with MF20, a monoclonal antibody against sarcomeric myosin heavy chain (MHC), was performed as described previously [7]. An anti-mouse immunoglobulin G conjugated with tetramethyl rhodamine isothiocyanate was used as the secondary antibody. The cell size of cardiomyocytes was measured by directly tracing the stained areas on a photograph.

[^{3}H]Phenylalanine incorporation. Protein synthesis was assessed by measuring the [^{3}H]phenylalanine incorporation as previously described [7]. Cardiac myocytes were cultured for 2 days without serum and then incubated for 24h with AngII, ET-1 or vehicle. [^{3}H]Phenylalanine (1.0 μCi/ml) was added 3h before the harvest. Cells were washed three times with ice-cold phosphate-buffered saline (PBS), incubated 30min with 1ml of 10% trichloroacetic acid, and washed twice with PBS. Precipitates were solubilized for 30min in 800μl of 1N NaOH, and radioactivity was measured by liquid scintillation spectroscopy.

Northern blot analysis. Total cellular RNA was extracted from cardiac myocytes by acid-guanidine phenol–chloroform method. Ten micrograms of total RNA was size-fractionated by 1.2% agarose gels and transferred to nylon membranes. Northern blot analyses were performed using the *c-fos* and *ANP* cDNA as probes as described previously [26,31]. The cDNA of rat *MKP-1* was isolated by the polymerase chain reaction method with a pair of primers corresponding to the amino acids 174–181 and 342–349.

Transfection and reporter gene assay. The luciferase reporter plasmids (3 μg/dish) containing ~1800bp 5′ flanking region of the *brain natriuretic peptide* (*BNP*) gene (a kind gift from Dr. Y. Saito, Kyoto) were transiently transfected into cultured cardiac myocytes using standard calcium phosphate method. Cells were washed with PBS at 12h after transfection and culture medium was changed to the medium containing 0.1% FBS. After 24h of serum starvation, cells were treated with various reagents. Cells were harvested at 48h after stimulation in 150μl of extraction buffer (100mM tricine, 10mM $MgSO_4$, 2mM EDTA, pH 7.8, and 1mM dithiothreitol) and luciferase activities were measured by Berthold Lumat LB9501 luminometer. Next, 1μg of luciferase reporter plasmids containing the human *c-fos* promoter

(pFC2) [32] or rat β *myosin heavy chain* (*βMHC*) promoter (−354 to +33) [33] and 3 μg of *MKP-1* expression plasmid DNA were co-transfected into cultured cardiac myocytes using lipofectin, Tfx-50 (Promega, WI, USA), according to the manufacturer's instructions. At 4 h after the transfection, the culture medium was changed to 0.1% FCS-containing DMEM and 24 h later, cardiac myocytes were exposed to 10^{-6} M Ang II for 4 h. Differences in transfection efficiency were corrected by β-galactosidase activities of co-transfected *SV40-βgal* plasmids (0.5 μg/dish).

Immunoprecipitation and Western blot analysis. Cardiomyocytes were lysed with lysis buffer (1% Triton X-100, 50 mM Tris–HCl, pH 7.6, 150 mM NaCl, 100 μM sodium orthovanadate, 1 mM EDTA, 1 mM phenylmethylsulfonyl fluoride PMSF, and 1 mM aprotinin) and protein extract was immunoprecipitated with a polyclonal anti-MKP-1 antibody. Immunoprecipitates were subjected to SDS–PAGE and immunoblotted with the same anti-MKP-1 antibody. The anti-rabbit IgG conjugated with horseradish peroxidase was used as the secondary antibody and immune complexes were visualized using the ECL detection kit according to the manufacturer's directions.

Assay of ERK activity. The activity of ERKs was examined by "in gel assay" using MBP-containing gel as described previously [7]. In brief, cells were lysed with 100 ml Buffer A (25 mM Tris–HCl, pH 7.4, 25 mM NaCl, 1 mM sodium orthovanadate, 10 mM NaF, 10 mM sodium pyrophosphate, 10 nM okadaic acid, 0.5 mM EGTA, and 1 mM PMSF) and 25 μl of cell lysates was applied to an SDS–polyacrylamide gel containing 0.5 mg/ml MBP. ERKs in the gel were denatured in 6 M guanidine–HCl and renatured in 50 mM Tris–HCl, pH 8.0, containing 0.04% Triton X-100, and 5 mM of 2-mercaptoethanol. The activity of ERKs was assayed by incubating the gel with [γ-^{32}P]ATP. After incubation, the gel was washed, dried, and subjected to autoradiography.

Statistical analysis. All results are expressed as means ± SEM. One-way ANOVA and Fisher's exact test for post hoc analyses carried out multiple comparisons among three or more groups. A value of $P < 0.05$ was considered statistically significant.

Results

ANP inhibited AngII- or ET-1-induced cardiomyocyte hypertrophy

To examine whether ANP directly inhibits the development of cardiomyocyte hypertrophy, cultured cardiomyocytes were pretreated with ANP and then stimulated by AngII or ET-1. AngII or ET-1 enhanced the cell size of cardiomyocytes by approximately 2.6- or 3.2-fold, respectively (Figs. 1A and B). Pretreatment of cardiomyocytes with ANP (10^{-7} M) for 2 h significantly inhibited the AngII- or ET-1-induced increase in the cell size (Figs. 1A and B). A cGMP analog 8-Br-cGMP (10^{-3} M) also significantly blocked the vasoactive peptide-induced increase in the cell size (Fig. 1B). We also examined the protein synthesis in cardiomyocytes which were pretreated with ANP and subsequently stimulated by the vasoactive peptides. AngII or ET-1 stimulation increased the phenylalanine incorporation in cardiomyocytes by approximately 1.5- or 1.8-fold, respectively (Fig. 1C), which is consistent with previous results [5,7,9]. Pretreatment with ANP significantly reduced the AngII- or ET-1-induced increase in phenylalanine incorporation (Fig. 1C). 8-Br-cGMP also significantly inhibited the vasoactive peptide-induced phenylalanine incorporation (Fig. 1C). To confirm the relationship between ANP and cGMP in cardiomyocytes, we examined the concentrations of cGMP in the culture media after treatment of cardiomyocytes with ANP. The ANP treatment increased the cGMP concentrations in a dose-dependent manner, suggesting that ANP induces the cGMP generation, and secretion from cardiomyocytes (Fig. 1D). Furthermore, we investigated whether changes in the cGMP activity influence the inhibitory actions of ANP on vasoactive peptide-induced hypertrophic responses. Pretreatment with a selective inhibitor of the cGMP-specific phosphodiesterase (ZAPRINAST), which increases the cGMP concentration by blocking its metabolism, enhanced the inhibitory effect of ANP on AngII- or ET-1- induced increase in phenylalanine incorporation (Fig. 1E). On the other hand, pretreatment with a cGMP-dependent protein kinase inhibitor (KT5823), which blocks signals from cGMP, suppressed it (Fig. 1E). These effects of ZAPRINAST or KT5823 on actions of ANP were statistically significant in case of ET-1, though not of Ang II (Fig. 1E). These results suggest that ANP has a direct inhibitory effect on vasoactive peptide-induced cardiomyocyte hypertrophy in a cGMP-dependent manner.

ANP inhibited AngII- or ET-1-induced hypertrophic responses in cardiomyocytes

We next examined the effects of ANP on AngII- or ET-1-induced hypertrophic responses such as specific gene expressions. AngII induced expression of the *c-fos* gene in cardiac myocytes and the induction was inhibited by the pretreatment with 10^{-7} M ANP (Fig. 2A). The inhibitory effect of ANP on the *c-fos* gene induction was mimicked by the pretreatment with 10^{-3} M 8-Br-cGMP (Fig. 2A). We also examined the effects of ANP on the induction of fetal cardiac genes by AngII or ET-1. Both AngII and ET-1 increased the expression levels of the *ANP* gene, and pretreatment with ANP or 8-Br-cGMP inhibited AngII- or ET-1-induced increase in the *ANP* mRNA levels (Fig. 2B). To elucidate whether ANP inhibits the induction of fetal genes at the transcriptional level, we examined the effects of ANP on the *BNP* promoter activity. AngII or ET-1 activated the *BNP* promoter by approximately 2.5- or 3.5-fold, respectively (Fig. 2C). This transcriptional activation was significantly inhibited by the pretreatment of cardiomyocytes with ANP (10^{-7} M) or 8-Br-cGMP (10^{-3} M), although ANP or 8-Br-cGMP had no effects on the basal promoter activity of *BNP* (Fig. 2C). These results suggest that ANP inhibits the vasoactive peptide-induced reprogramming of gene expression in cardiomyocytes in a cGMP-dependent manner.

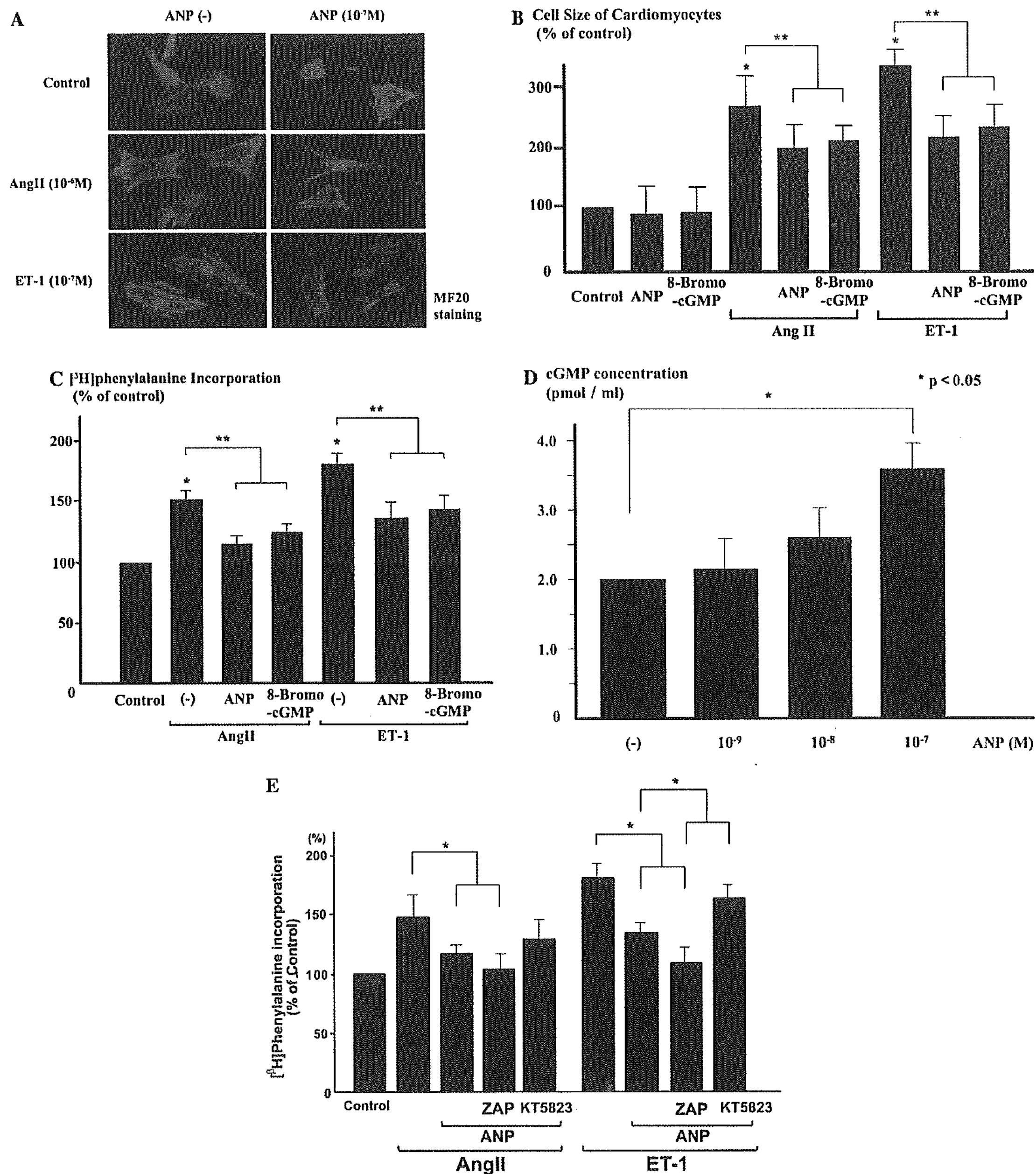

Fig. 1. ANP inhibited AngII- or ET-1-induced increase in the cell size and the protein synthesis of cardiomyocytes. (A,B) After pretreatment with ANP (10^{-7} M) or 8-Br-cGMP (10^{-3}M) for 2h, cultured cardiomyocytes were stimulated with 10^{-6}M AngII or 10^{-7}M ET-1 for 24h and then the cells were immunostained with MF20, an anti-sarcomeric MHC antibody, 24h later. The cell size of cardiomyocytes was measured by directly tracing the stained areas on a photograph. Data represent the average percentages against the control (=100%, vehicle) from three independent experiments (mean ± SE). Statistical differences ($P < 0.05$) between the non-treated control and the Ang II or ET-1 treatment are denoted by *, and those between no pretreatment and ANP or 8-Br-cGMP pretreatment are shown by **. (C) After pretreatment with ANP (10^{-7}M) or 8-Br-cGMP (10^{-3}M) for 2h and subsequent stimulation with AngII (10^{-6}M) or ET-1 (10^{-7}M) for 24h, [^{3}H]phenylalanine (1 μCi/ml) was added 3h before harvest. The effects of ANP or 8-Br-cGMP on the protein synthesis were evaluated by measuring the [^{3}H]phenylalanine incorporation. The total radioactivity of incorporated [^{3}H]phenylalanine was determined by liquid scintillation counting. Data represent the average percentages against the control (=100%, vehicle) from three independent experiments (means ± SE). Statistical differences ($P < 0.05$) between the non-treated control and the AngII or ET-1 treatment are denoted by *, and those between no pretreatment and ANP or 8-Br-cGMP pretreatment are shown by **. (D) After serum starvation of cultured cardiomyocytes with 0.1% FBS for 48h and subsequent treatment with ANP at indicated concentrations for 24h, the concentrations of cGMP in the culture media were examined. Statistical differences ($P < 0.05$) from the non-treated control are denoted by *. (E) After pretreatment with ANP (10^{-7}M) along with ZAPRINAST (ZAP) and KT5823 (10^{-8}M each) for 2h and subsequent stimulation with AngII (10^{-6}M) or ET-1 (10^{-7}M) for 24h, [^{3}H]phenylalanine (1 μCi/ml) was added 3h before harvest. The evaluation of the [^{3}H]phenylalanine incorporation is similar to that in (C).

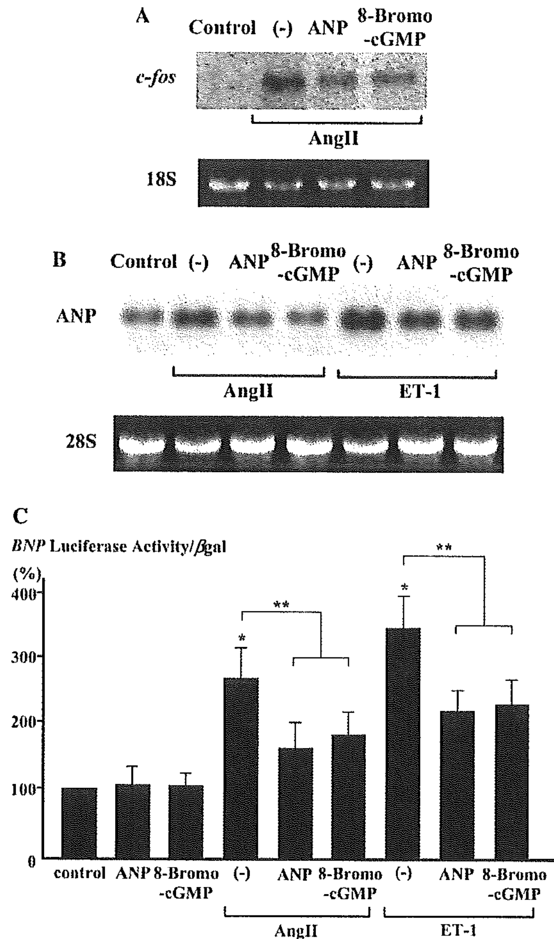

Fig. 2. ANP inhibited AngII- or ET-1-induced hypertrophic responses in cardiomyocytes. (A) Expression of the *c-fos* gene was examined by Northern blot analysis. Cardiomyocytes were pretreated for 2h with ANP (10^{-7}M) or 8-Br-cGMP (10^{-3}M) and stimulated with AngII (10^{-6}M) for 30min. A representative autoradiogram is shown. (B) The *ANP* gene expression was examined by Northern blot analysis. Cardiomyocytes were pretreated for 24h with ANP (10^{-7}M) or 8-Br-cGMP (10^{-3}M) and stimulated with AngII (10^{-6}M) or ET-1 (10^{-7}M) for 2h. A representative autoradiogram is shown. (C) The *BNP* promoter activity was examined by transient transfection assay. The results are indicated as means ± SEM of three independent experiments ($n = 9$) compared with unstimulated controls (100%). Statistical differences ($P < 0.05$) between the non-treated control and the AngII or ET-1 treatment are denoted by *, and those between no pretreatment and the ANP or 8-Br-cGMP pretreatment are shown by **.

ANP decreased basal activities of ERKs in cardiomyocytes in a cGMP-dependent manner

We next examined the effects of ANP on MAPK, which has been reported to be important for the induction of cardiac hypertrophy [10,11]. The in-gel assay revealed that basal activities of both 44kDa (ERK1) and 42kDa (ERK2) ERKs were reduced by the treatment with ANP in a dose-dependent manner (Fig. 3A) and a significant decrease in ERK activities was observed at 60min and reached the minimum level at 120min after the 10^{-7}M ANP treatment (Fig. 3B). 8-Br-cGMP decreased basal activities of ERKs in a dose-dependent manner (Fig. 3C) with the same time course as ANP (Fig. 3D). These results suggest that ANP represses the basal ERK activity in a cGMP-dependent manner in cardiac myocytes.

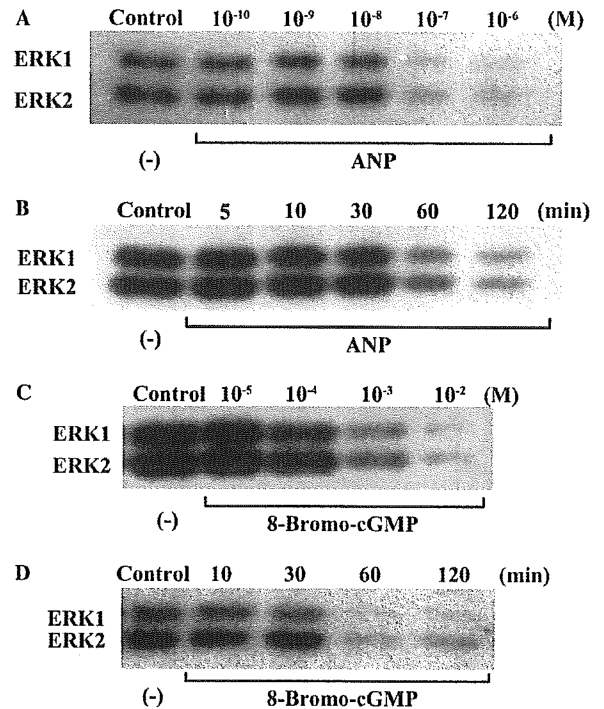

Fig. 3. ANP suppressed basal activities of ERKs in cardiomyocytes. (A) Cultured cardiomyocytes were treated with various concentrations of ANP (10^{-10}–10^{-6}M) for 2h and the activities of ERKs were measured by the in-gel kinase assay described in "Materials and methods." (B) Cultured cardiomyocytes were treated with 10^{-7} M ANP and ERK activities were examined for indicated periods of time. (C) Cultured cardiomyocytes were treated with various concentrations of 8-Br-cGMP (10^{-5}–10^{-2}M) for 2h and the activities of ERKs were measured. (D) Cultured cardiomyocytes were treated with 8-Br-cGMP (10^{-3}M) and ERK activities were examined for indicated periods of time. Representative autoradiograms are shown.

ANP inhibited vasoactive peptide-induced activation of MAPKs in a cGMP-dependent manner

We next examined whether ANP represses the vasoactive peptide-induced activation of MAPK. Treatment of cardiomyocytes with 10^{-6}M AngII or 10^{-7}M ET-1 for 10min markedly increased the ERK activity as reported before [7,9]. This vasoactive peptide-induced increase in the ERK activity was significantly inhibited by the pretreatment with 10^{-7}M

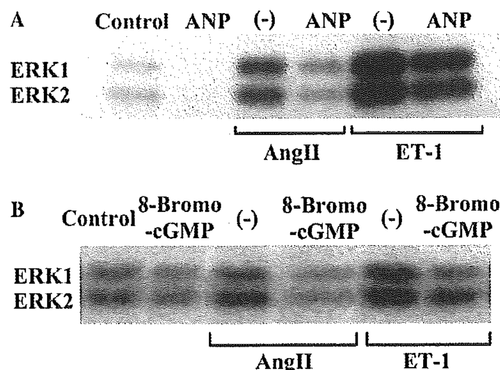

Fig. 4. ANP inhibited AngII- or ET-1-induced activation of MAPK in cardiomyocytes. (A) Cultured cardiomyocytes were pretreated with ANP (10^{-7}M) for 2h and stimulated with AngII or ET-1 for 10min. ERK activities were measured by the in-gel kinase assay. (B) Cultured cardiomyocytes were stimulated with AngII or ET-1 for 10min and the effects of 8-Br-cGMP (10^{-3}M) pretreatment for 2h on ERK activities were examined by the in-gel kinase assay. Representative autoradiograms are shown.

ANP for 2h (Fig. 4A). The effects of 8-Br-cGMP on vasoactive peptide-induced ERK activation were also examined. Pretreatment of cardiomyocytes with 10^{-3}M 8-Br-cGMP decreased the AngII- or ET-1-induced ERK activation by approximately 70% and 60%, respectively (Fig. 4B).

ANP induced MKP-1 expression in cardiomyocytes

MAPK is inactivated by a dual phosphatase, MKP-1 [21], and the induction of MKP-1 has been implicated in the growth-inhibitory effects of ANP in mesangial cells [20]. To elucidate the mechanism by which ANP inhibits the development of cardiomyocyte hypertrophy, we examined whether MKP-1 is induced in cardiomyocytes by ANP. ANP significantly increased expression levels of the *MKP-1* gene and the mRNA levels of *MKP-1* peaked at 30min and returned to the basal level at 120min after the treatment with ANP (10^{-7}M) (Fig. 5A). 8-Br-cGMP (10^{-3}M) also induced MKP-1 by the same time course (Fig. 5A). The protein content of MKP-1 was also examined by Western blot analysis. The MKP-1 protein was dramatically induced by ANP or 8-Br-cGMP with its peak at 120min after the treatment (Fig. 5B). These results clearly indicate that ANP induces expression of MKP-1 in cardiomyocytes in a cGMP-dependent manner.

MKP-1 blocked vasoactive peptide-induced hypertrophic responses

To elucidate the significance of the increase in the *MKP-1* gene expression, we examined the effects of

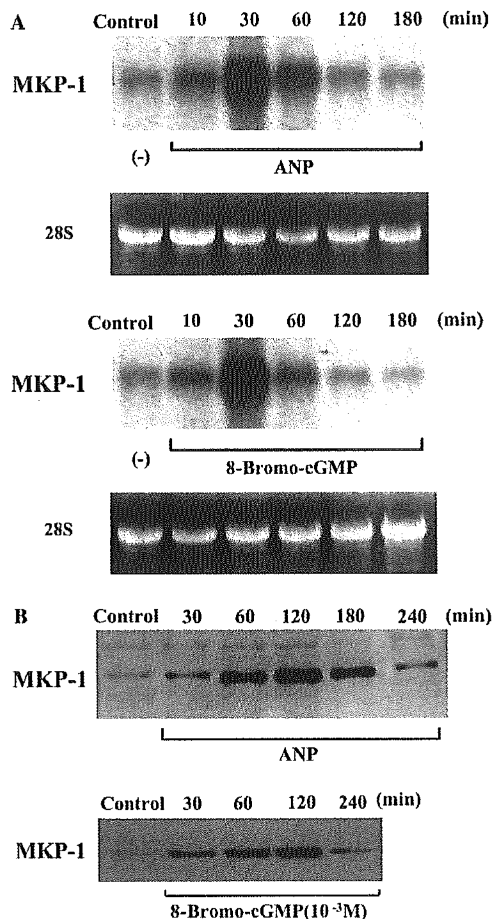

Fig. 5. ANP induced expression of MKP-1 in cardiomyocytes. (A) Cultured cardiomyocytes were treated with ANP or 8-Br-cGMP for indicated periods of time and expression of the *MKP-1* mRNA was examined by Northern blot analysis. (B) Cultured cardiomyocytes were treated with ANP or 8-Br-cGMP for the indicated periods of time and the protein content of MKP-1 was examined by immunoblot analysis. Representative autoradiograms are shown.

overexpression of the *MKP-1* gene on hypertrophic responses such as induction of the *c-fos* and *βMHC* genes. We co-transfected *c-fos* or *βMHC* promoter-containing luciferase reporter plasmids and *MKP-1* expression plasmids into the cultured cardiomyocytes, and examined the luciferase activity after stimulation with AngII. AngII activated the *c-fos* gene transcription in cardiomyocytes (Fig. 6A). Overexpression of the *MKP-1* mRNA significantly suppressed the AngII-induced increase in the *c-fos* gene transcription as well as the non-treated, basal transcription (Fig. 6A). AngII also increased the luciferase activity of the *βMHC* reporter gene and overexpression of *MKP-1* significantly suppressed the AngII-induced increase in the *βMHC* gene transcription (Fig. 6B). Furthermore, overexpression of *MKP-1* significantly suppressed AngII- or ET-1-induced increase in

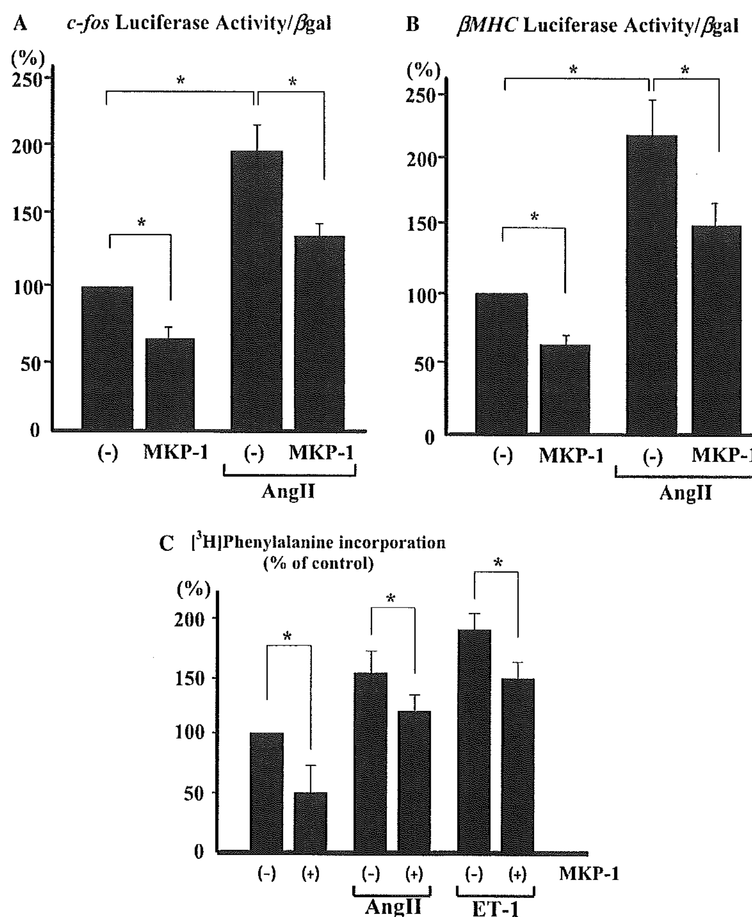

Fig. 6. MKP-1 blocked AngII- or ET-1-induced hypertrophic responses in cardiomyocytes. (A,B) One microgram of MKP-1 plasmid DNA was co-transfected with 1 μg of *c-fos* (A) or *βMHC* (B) luciferase reporter plasmids into cultured cardiomyocytes using lipofectin, Tfx-50. At 4 h after the transfection, the culture medium was changed to 0.1% FBS-containing DMEM. After this serum starvation for 24 h, cardiomyocytes were incubated with Ang II (10^{-6} M) for 4 h. Luciferase activities were measured using a luminometer and the data are shown as means ± SEM of three independent assays ($n = 18$) ($^*P < 0.05$). (C) After the transfection and the starvation same as those in (A,B), cardiomyocytes were incubated with Ang II (10^{-6} M) and ET-1 (10^{-7} M) for 24 h. [^{3}H]Phenylalanine (1 μCi/ml) was added 3 h before harvest. The evaluation of the [^{3}H]phenylalanine incorporation is similar to that in Fig. 1C. Statistical differences ($P < 0.05$) from the non-transfected control are denoted by *.

phenylalanine incorporation (Fig. 6C). These findings suggest that an increase in the *MKP-1* mRNA levels inhibits vasoactive peptide-induced hypertrophic responses such as an increase in protein synthesis and specific gene expressions.

Discussion

In the present study, we have obtained several results as follows. (i) ANP directly inhibits the vasoactive peptide-induced increase in the cell size and the protein synthesis of cardiomyocytes through the cGMP-dependent pathway. (ii) ANP also inhibits the vasoactive peptide-induced hypertrophic responses such as reprogramming of gene expressions and activation of MAPK. (iii) ANP upregulates expression of MKP-1 in cardiomyocytes. (iv) Overexpression of *MKP-1* inhibits the vasoactive peptide-induced hypertrophic responses.

ANP was originally identified as a natriuretic and diuretic peptide predominantly produced and secreted from atrial cells. Many studies demonstrated that ANP regulates sodium and water homeostasis via changes in the glomerular filtration rate and inhibition of the renin and aldosterone secretion [13]. In addition to these effects on the circulatory system, ANP has been shown to have a direct vasorelaxing effect which counteracts the vasoconstrictive factors such as AngII and ET-1 [13]. Moreover, it has recently been demonstrated that ANP acts as a growth-inhibitory factor that antagonizes the growth-promoting effects of AngII or ET-1 in various cell types including vascular smooth muscle

cells, glomerular mesangial cells, astrocytes, endothelial cells, and cardiac fibloblasts [14–19]. These findings suggest that ANP antagonizes various effects of vasoactive and/or growth-promoting factors. We therefore hypothesized that ANP might antagonize cardiomyocyte hypertrophy-promoting effects of vasoactive peptides. In the present study, in fact, ANP inhibited the AngII- or ET-1-induced increase in protein synthesis and hypertrophic responses such as expression of *c-fos* and fetal type genes and activation of MAPK in cardiomyocytes.

ANP and the other natriuretic peptides function through a family of membrane receptors called natriuretic peptide receptors, NPR-A, NPR-B, and NPR-C [13]. NPR-A and NPR-B have three domains, an extracellular ligand-binding domain, a single transmembrane domain, and an intracellular domain. An intracellular domain is consisting of a kinase domain and a guanylyl cyclase domain, which generates cGMP upon ligand binding [13]. On the other hand, NPR-C or clearance receptor contains the extracellular and transmembrane domains but lacks the intracellular domain, and is thought to be mainly responsible for the internalization and degradation of ligands [13]. Our present data strongly suggest that the anti-hypertrophic actions of ANP are mediated by guanylyl cyclase-linked NPR-A because a cGMP analog 8-Br-cGMP showed the effects similar to ANP and also because ANP exhibits relatively higher binding affinity for NPR-A than for NPR-B. Another recent report demonstrated that the inhibitory action of ANP on hypertrophic response was not suppressed by a cGMP-dependent protein kinase inhibitor KT5823, implying the involvement of additional cGMP-independent pathways [34]. This result and our present results are controversial, which may be at least partially due to differences in cardiomyocytes used in assays (adult vs. neonatal) and the ways how to stimulate them (concentration, duration, etc.). Nevertheless, we consider our data clearly and for the first time demonstrated a series of evidence that the cGMP analog mimicked the effects of ANP on vasoactive peptide-induced cardiomyocyte hypertrophy, indicating the importance of the cGMP-dependent pathway for this anti-hypertrophic action of ANP. The growth-inhibitory effects of ANP on glomerular mesangial cells [20] and vascular smooth muscle cells [18] are also thought to be mediated by cGMP-dependent pathways, although the anti-proliferative actions of ANP on astrocytes [19] are reported to be mediated by clearance receptors, suggesting that modes of inhibitory actions of ANP may depend on cell types nonetheless.

Although the mechanism by which AngII or ET-1 induces cardiomyocyte hypertrophy is not fully understood, protein kinases especially the MAPK family have been reported to play a pivotal role in the development of cardiac hypertrophy [10,11,27–30]. Three subfamilies of MAPKs such as ERKs, JNK, and p38MAPK have been reported to be involved in cardiac hypertrophy as follows. (i) Hypertrophic stimuli such as AngII and ET-1 activate all three members of MAPKs [5–7,9,26,29]. (ii) Anti-sense oligonucleotides against ERKs inhibit the phenylephrine-induced increase in cell size [12]. (iii) Selective activation of JNK by a constitutively active form of MKK7/JNKK2 leads to cardiomyocyte hypertrophy [30]. (iv) Activation of p38MAPK induces cardiomyocyte hypertrophy while that of JNK exhibits inhibitory effects [27]. (v) p38MAPK is necessary for the maintenance of hypertrophic response in a longer period but not for the immediate morphological responses [29]. Taken together, although precise roles of individual MAPKs are still controversial at present, these results suggest that activation of the MAPK pathways plays a critical role in the development of cardiomyocyte hypertrophy. In this respect, MKP-1, the recently identified dual protein phosphatase with selectivity for MAPKs, is of quite interest as a negative regulator of the MAPK pathways [21]. MKP-1 has been shown to be widely expressed in various cell types and to be capable of dephosphorylating phosphothreonine and phosphotyrosine residues of ERKs, JNK, and p38MAPK [21,24,32]. Because expression of MKP-1 is rapidly induced by many growth factors and cytokines that also induce activation of ERKs, JNK, and p38MAPK, MKP-1 has been implicated for the feedback loop serving to downregulate the MAPK activities in response to external stimuli [21,24,32]. Recently, MKP-1 has been reported to be induced by ANP in glomerular mesangial cells [20]. MKP-1 was also induced by ANP in cardiomyocytes in this study, although ANP did not activate ERKs in cardiomyocytes (data not shown). ANP also reduced the basal MAPK activity and inhibited vasoactive peptide-induced activation of MAPK in cardiomyocytes through the cGMP-dependent pathways. Taken together, our present study suggests that ANP inhibits the vasoactive peptide-induced cardiomyocyte hypertrophy at least in part by inhibiting activation of MAPK through upregulation of MKP-1.

In addition to the induction of MKP-1, there are possible mechanisms by which ANP inhibits the growth-promoting processes in various cell types. In astrocytes, ANP has been shown to inhibit ERKs by attenuating the MEK activity, although the precise signaling pathway leading to the inactivation of MEK remains to be identified [19]. In mesangial cells, ANP inhibits the ET-1-induced JNK activation possibly by attenuating the ET-1-induced increase in intracellular Ca^{2+} concentration [33]. It has been reported that ANP inhibits the norepinephrine-induced growth of cardiac myocytes by a cGMP-mediated inhibition of norepinephrine-stimulated Ca^{2+} influx [35]. Although MKP-1 was strongly induced in cardiomyocytes by ANP, we cannot rule out

the possibilities that some other mechanisms are also involved in the growth-inhibitory effects of ANP in cardiomyocytes.

Although a variety of molecules that promote the development of cardiac hypertrophy have been well examined [3–8], little is known about the molecules that inhibit cardiac hypertrophy. ANP is quite unique in that it exhibits growth-inhibitory effects on cardiomyocytes. Simultaneous induction of both growth-promoting and growth-inhibiting factors in the myocardium suggests that cardiac growth in response to hemodynamic overload is controlled by complex regulatory mechanisms. Although the precise mechanism by which ANP inhibits the development of cardiac hypertrophy remains to be further clarified, understanding the physiological and pathological actions of ANP on cardiac cells may allow the development of novel therapeutic strategies for modulating the hypertrophy of cardiomyocytes and the overall remodeling of the myocardium.

References

[1] A.M. Katz, Cardiomyopathy of overload. A major determinant of prognosis in congestive heart failure, N. Engl. J. Med. 322 (1990) 100–110.

[2] D. Levy, R.J. Garrison, D.D. Savage, W.B. Kannel, W.P. Castelli, Prognostic implications of echocardiographically determined left ventricular mass in the Framingham heart study, N. Engl. J. Med. 332 (1990) 1561–1566.

[3] I. Komuro, Y. Yazaki, Control of cardiac gene expression by mechanical stress, Annu. Rev. Physiol. 55 (1993) 55–75.

[4] K.M. Baker, J.F. Aceto, Angiotensin II stimulation of protein synthesis and cell growth in chick heart cells, Am. J. Physiol. 259 (1990) H610–H618.

[5] J. Sadoshima, Z. Qiu, J.P. Morgan, S. Izumo, Angiotensin II and other hypertrophic stimuli mediated by G protein-coupled receptors activate tyrosine kinase, mitogen-activated protein kinase, and 90-kD S6 kinase in cardiac myocytes: the critical role of Ca^{2+}-dependent signaling, Circ. Res. 76 (1995) 1–15.

[6] M. Kojima, I. Shiojima, T. Yamazaki, I. Komuro, Y. Zou, W. Ying, T. Mizuno, K. Ueki, K. Tobe, T. Kadowaki, R. Nagai, Y. Yazaki, Angiotensin II receptor antagonist TCV-116 induces regression of hypertensive left ventricular hypertrophy in vivo and inhibits the intracellular signaling pathway of stretch-mediated cardiomyocyte hypertrophy in vivo, Circulation 89 (1994) 2204–2211.

[7] T. Yamazaki, I. Komuro, S. Kudoh, Y. Zou, I. Shiojima, T. Mizuno, H. Takano, Y. Hiroi, K. Ueki, K. Tobe, T. Kadowaki, Y. Yazaki, Angiotensin II partly mediates mechanical stress-induced cardiac hypertrophy, Circ. Res. 77 (1995) 258–265.

[8] H. Ito, M. Hiroe, Y. Hirata, H. Fujisaki, S. Adachi, H. Akimoto, Y. Ohta, F. Marumo, Endothelin ETA receptor antagonist blocks cardiac hypertrophy provoked by hemodynamic overload, Circulation 89 (1994) 2198–2203.

[9] T. Yamazaki, I. Komuro, S. Kudoh, Y. Zou, I. Shiojima, Y. Hiroi, T. Mizuno, K. Maemura, H. Kurihara, R. Aikawa, H. Takano, Y. Yazaki, Endothelin-1 is involved in mechanical stress-induced cardiomyocyte hypertrophy, J. Biol. Chem. 271 (1996) 3221–3228.

[10] J. Thorburn, J.A. Frost, A. Thorburn, Mitogen-activated protein kinases mediate changes in gene expression, but not cytoskeletal organization associated with cardiac muscle cell hypertrophy, J. Cell Biol. 126 (1994) 1565–1572.

[11] J. Thorburn, M. Carlson, S.J. Mansour, K.R. Chien, N.G. Ahn, A. Thorburn, Inhibition of a signaling pathway in cardiac muscle cells by active mitogen-activated protein kinase kinase, Mol. Biol. Cell. 6 (1995) 1479–1490.

[12] P.E. Glennon, S. Kadoura, E.M. Sale, G.J. Sale, S.J. Fuller, P.H. Sugden, Depletion of mitogen-activated protein kinase using an antisense oligodeoxynucleotide approach downregulates the phenylephrine-induced hypertrophic response in rat cardiac myocytes, Circ. Res. 78 (1996) 954–961.

[13] H. Ruskoaho, Atrial natriuretic peptide: synthesis, release, and metabolism, Pharmcol. Rev. 44 (1992) 479–602.

[14] U.C. Garg, A. Hassid, Nitric oxide-generating vasodilators and 8-bromo-cyclic guanosine monophosphate inhibit mitogenesis and proliferation of cultured rat vascular smooth muscle cells, J. Clin. Invest. 83 (1989) 1774–1777.

[15] M. Kohno, M. Ikeda, M. Johchi, T. Horio, K. Yasunari, N. Kurihara, T. Takeda, Interaction of PDGF and natriuretic peptides on mesangial cell proliferation and endothelin secretion, Am. J. Physiol. 265 (1993) E673–E679.

[16] R. Morishita, G.H. Gibbons, R.E. Pratt, N. Tomita, Y. Kaneda, T. Ogihara, V.J. Dzau, Autocrine and paracrine effects of atrial natriuretic peptide gene transfer on vascular smooth muscle and endothelial cellular growth, J. Clin. Invest. 94 (1995) 824–829.

[17] L. Cao, D.G. Gardner, Natriuretic peptides inhibit DNA synthesis in cardiac fibroblasts, Hypertension 25 (1995) 227–234.

[18] S.M. Yu, L.M. Hung, C.C. Lin, cGMP-elevating agents suppress proliferation of vascular smooth muscle cells by inhibiting the activation of epidermal growth factor signaling pathway, Circulation 95 (1997) 1269–1277.

[19] B.A. Prins, M.J. Weber, R.M. Hu, A. Pedram, M. Daniels, E.R. Levin, Atrial natriuretic peptide inhibits mitogen-activated protein kinase through the clearance receptor. Potential role in the inhibition of astrocyte proliferation, J. Biol. Chem. 271 (1996) 14156–14162.

[20] T. Sugimoto, M. Haneda, M. Togawa, M. Isono, T. Shikano, S. Araki, T. Nakagawa, A. Kashiwagi, K.L. Guan, R. Kikkawa, Atrial natriuretic peptide induces the expression of MKP-1, a mitogen-activated protein kinase phosphatase, in glomerular mesangial cells, J. Biol. Chem. 271 (1996) 544–547.

[21] H. Sun, C.H. Charles, L.F. Lau, N.K. Tonks, MKP-1 (3CH134), an immediate early gene product, is a dual specificity phosphatase that dephosphorylates MAP kinase in vivo, Cell 75 (1993) 487–493.

[22] S.J. Fuller, E.L. Davies, J. Gillespie-Brown, H. Sun, N.K. Tonks, Mitogen-activated protein kinase phosphatase 1 inhibits the stimulation of gene expression by hypertrophic agonists in cardiac myocytes, Biochem. J. 323 (1997) 313–319.

[23] H. Sun, N.K. Tonks, D. Bar-Sagi, Inhibition of Ras-induced DNA synthesis by expression of the phosphatase MKP-1, Science 266 (1994) 285–288.

[24] Y. Liu, M. Gorospe, C. Yang, N.J. Holbrook, Role of mitogen-activated protein kinase phosphatase during the cellular response to genotoxic stress. Inhibition of c-Jun N-terminal kinase activity and AP-1-dependent gene activation, J. Biol. Chem. 270 (1995) 8377–8380.

[25] I. Komuro, S. Kudoh, T. Yamazaki, Y. Zou, I. Shiojima, Y. Yazaki, Mechanical stretch activates the stress-activated protein kinases in cardiac myocytes, FASEB J. 10 (1996) 631–636.

[26] S. Kudoh, I. Komuro, Y. Hiroi, Y. Zou, K. Harada, T. Sugaya, N. Takekoshi, K. Murakami, T. Kadowaki, Y. Yazaki, Mechanical stretch induces hypertrophic responses in cardiac myocytes of angiotensin II type 1a receptor knockout mice, J. Biol. Chem. 273 (1998) 24037–24043.

[27] S. Nemoto, Z. Sheng, A. Lin, Opposing effects of Jun kinase and p38 mitogen-activated protein kinases on cardiomyocyte hypertrophy, Mol. Cell. Biol. 18 (1998) 3518–3526.

[28] D. Zechner, D.J. Thuerauf, D.S. Hanford, P.M. McDonough, C.C. Glembotski, A role for the p38 mitogen-activated protein kinase pathway in myocardial cell growth, sarcomeric organization, and cardiac-specific gene expression, J. Cell Biol. 139 (1997) 115–127.

[29] A. Clerk, A. Michael, P.H. Sugden, Stimulation of the p38 mitogen-activated protein kinase pathway in neonatal rat ventricular myocytes by the G protein-coupled receptor agonists, endothelin-1 and phenylephrine: a role in cardiac myocyte hypertrophy?, J. Cell Biol. 142 (1998) 523–535.

[30] Y. Wang, B. Su, V.P. Sah, J.H. Brown, J. Han, K.R. Chien, Cardiac hypertrophy induced by mitogen-activated protein kinase kinase 7, a specific activator for c-Jun NH2-terminal kinase in ventricular muscle cells, J. Biol. Chem. 273 (1998) 5423–5426.

[31] K. Harada, I. Komuro, I. Shiojima, D. Hayashi, S. Kudoh, T. Mizuno, K. Kijima, H. Matsubara, T. Sugaya, K. Murakami, Y. Yazaki, Pressure overload induces cardiac hypertrophy in angiotensin II type 1A receptor knockout mice, Circulation 97 (1998) 1952–1959.

[32] D.R. Alessi, C. Smythe, S.M. Keyse, The human CL100 gene encodes a Tyr/Thr-protein phosphatase which potently and specifically inactivates MAP kinase and suppresses its activation by oncogenic ras in *Xenopus* oocyte extracts, Oncogene 8 (1993) 2015–2020.

[33] M. Isono, M. Haneda, S. Maeda, M. Omatsu-Kanbe, R. Kikkawa, Atrial natriuretic peptide inhibits endothelin-1-induced activation of JNK in glomerular mesangial cells, Kidney Int. 53 (1998) 1133–1142.

[34] A.C. Rosenkranz, R.L. Woods, G.J. Dusting, R.H. Ritchie, Antihypertrophic actions of the natriuretic peptides in adult rat cardiomyocytes: importance of cyclic GMP, Cardiovasc. Res. 57 (2003) 515–522.

[35] C. Angelino, M.T. Cynthia, T. Nobuyuki, L.F.C. Donny, S.C. Wilson, Nitric oxide, atrial natriuretic peptide, and cyclic GMP inhibit the growth-promoting effects of norepinephrine in cardiac myocytes and fibroblasts, J. Clin. Invest. 101 (1998) 812–818.

ELSEVIER

Available online at www.sciencedirect.com

SCIENCE @ DIRECT®

Biochemical and Biophysical Research Communications 314 (2004) 849–853

BBRC

www.elsevier.com/locate/ybbrc

Role of Na^+–Ca^{2+} exchanger in myocardial ischemia/reperfusion injury: evaluation using a heterozygous Na^+–Ca^{2+} exchanger knockout mouse model

Masashi Ohtsuka,[a] Hiroyuki Takano,[a] Masashi Suzuki,[b] Yunzeng Zou,[a] Hiroshi Akazawa,[a] Masaji Tamagawa,[b] Koji Wakimoto,[c] Haruaki Nakaya,[b] and Issei Komuro[a,*]

[a] *Department of Cardiovascular Science and Medicine, Chiba University Graduate School of Medicine, 1-8-1 Inohana, Chuo-ku, Chiba 260-8670, Japan*
[b] *Department of Pharmacology, Chiba University Graduate School of Medicine, 1-8-1 Inohana, Chuo-ku, Chiba 260-8670, Japan*
[c] *Discovery Research Laboratory, Tanabe Seiyaku Co. Ltd., 3-16-89 Kashima, Yodogawa-ku, Osaka 532-8505, Japan*

Received 5 December 2003

Abstract

We used Na^+–Ca^{2+} exchanger (NCX) knockout mice to evaluate the effects of NCX in cardiac function and the infarct size after ischemia/reperfusion injury. The contractile function in NCX KO mice hearts was significantly better than that in wild type (WT) mice hearts after ischemia/reperfusion and the infarct size was significantly small in NCX KO mice hearts compared with that in WT mice hearts. NCX is critically involved in the development of ischemia/reperfusion-induced myocardial injury and therefore the inhibition of NCX function may contribute to cardioprotection against ischemia/reperfusion injury.
© 2003 Elsevier Inc. All rights reserved.

Keywords: Sodium–calcium exchanger; Knockout mouse; Heart; Ischemia/reperfusion injury

The Na^+–Ca^{2+} exchanger (NCX) is an important electrogenic transporter in maintaining calcium homeostasis in a variety of mammalian organs [1]. NCX catalyzes electrogenic exchange of Na^+ and Ca^{2+} across the plasma membrane in either the Ca^{2+}-efflux (the forward mode) or Ca^{2+}-influx (the reverse mode), depending on the electrochemical gradients of the substrate ions. In the heart, NCX plays an important role in excitation–contraction coupling as the dominant myocardial Ca^{2+}-efflux system [2]. On the other hand, the reverse mode of NCX is associated with in cytoplasmic Ca^{2+} levels in cardiomyocytes during digitalis treatment or ischemia/reperfusion [3]. It has been reported that NCX inhibitors and NCX antisense oligonucleotides protect the heart from ischemia/reperfusion injury [4,5]. However, two putative NCX inhibitors, KB-R7943 and SEA0400, have been reported to be not specific for NCX [6]. Therefore, it remains unclear whether NCX indeed plays a crucial role in mediating Ca^{2+} influx that leads to Ca^{2+} overload and cellular injury after myocardial ischemia, reperfusion injury. Using heterozygous NCX KO mice, we examined the role of NCX in myocardial ischemia/reperfusion injury.

* Corresponding author. Fax: +81-43-226-2557.
E-mail address: komuro-tky@umin.ac.jp (I. Komuro).

0006-291X/$ - see front matter © 2003 Elsevier Inc. All rights reserved.
doi:10.1016/j.bbrc.2003.12.165

Materials and methods

NCX KO mice. NCX knockout (KO) mice were generated as described previously [7]. Male heterozygous KO mice and wild type (WT) littermates 12 weeks old were used. All animal experiments were performed according to the *Guide for the Care and Use of Laboratory Animals* (NIH Publication No. 85-23, revised 1996).

Electrophysiology. Ventricular cells were prepared from adult mice hearts by standard enzymatic digestion [8]. Whole-cell membrane currents were recorded by the patch-clamp method and the current–voltage relationship was obtained by voltage clamp ramp pulses as described previously [9]. Under these conditions, the Ni^{2+}-sensitive current represents NCX current [10]. All data were acquired and analyzed by the pCLAMP (version 5.5; Axon Instrument) software.

Western blot analysis. Expression levels of dihydropyridine (DHP) receptor (L-type Ca^{2+} channel) and SR Ca^{2+}-ATPase 2 (SERCA2)

were analyzed by Western blot as described previously [11]. Briefly, tissue was homogenized in lysis buffer containing 25 mM Tris–HCl (pH 7.4), 25 mM NaCl, 0.5 mM EGTA, 10 mM sodium pyrophosphate, 1 mM sodium orthovanadate, 10 mM NaF, 10 nM okadaic acid, 1 mM PMSF, 20 μg/ml aprotinin, and 20 μg/ml leupeptin. Protein concentration was determined using a protein assay kit (Bio-Rad) and equal amounts of total protein (40 μg/lane) were separated on 8% SDS–polyacrylamide gel. Separated proteins were transferred to nitrocellulose membrane (Amersham Life Science). Membranes were incubated with anti-mouse dihydropyridine L-type Ca^{2+} channel α-2 subunit monoclonal antibody (Affinity Bioreagents) or anti-mouse SERCA2 monoclonal antibody (Affinity Bioreagents) at 4 °C overnight. After washing, the membranes were incubated with horseradish peroxidase-conjugated goat anti-mouse antibody for 1 h. Immunoreactive protein was visualized using an enhanced chemiluminescence detection kit (ECL, Amersham).

Ischemia/reperfusion. Hearts were excised from mice and connected to the perfusion cannula via the aorta as described previously [8]. Retrograde perfusion was maintained with Krebs–Henseleit solution. To evaluate the contractile function, a polyethylene film balloon was inserted into the cavity of the left ventricle through the left atrium. The balloon was filled with saline to adjust the baseline end-diastolic pressure to 5–10 mmHg. Hearts were subjected to no-flow, global ischemia by clamping the perfusion line. After 30 min of ischemia, the clamp was released and the hearts were reperfused for 120 min. Left ventricular developed pressure (LVDP) was designated as difference between systolic and diastolic pressures of the left ventricle. After 120 min, the heart was incubated for 5 min at 37 °C in a 1% solution of triphenyltetrazolium chloride (TTC). The sizes of infarcted area (pale) and viable ischemic–reperfused area (red) were measured by computed planimetry (Scion Image 1.62). Infarct size was calculated as described previously [12].

Statistics analysis. All data are presented as means ± SEM. Statistical analyses of the data were performed using Student's t test. Probability values less than 0.05 were considered to be significant.

Results

NCX current density and Western blot analysis

We previously reported that the protein content of NCX in NCX KO mice hearts was ~50% of that in WT mice hearts [13]. To elucidate the functional activity, we examined NCX current densities from −40 to 40 mV in WT ($n = 9$) and NCX KO ventricular cells ($n = 6$) (Fig. 1). The densities of the reverse mode of NCX at 40 mV in ventricular cells of KO mice (0.57 ± 0.07 pA/pF) were approximately half (55.4%) compared with those of WT mice (1.04 ± 0.14 pA/pF). These results suggest that the functional activity as well as the protein content of NCX in the myocardium of NCX KO mice is approximately half of those of WT mice.

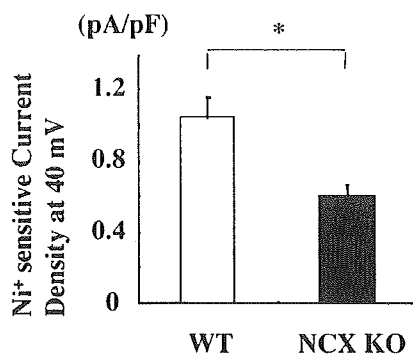

Fig. 1. NCX current densities. The densities of the reverse mode of NCX at 40 mV in ventricular myocytes isolated from WT ($n = 9$) and NCX KO mice hearts ($n = 6$). Values are expressed as means ± SEM. *$p < 0.05$ vs. WT mice.

Western blot analysis revealed that there was no difference in the protein levels of L-type Ca^{2+} channel and SERCA2 between the two groups (data not shown).

Mechanical function of hearts before and after ischemia/reperfusion

There were no significant differences in the basal hemodynamic parameters including heart rate, left ventricular pressure, end-diastolic pressure, and positive and negative dP/dt, between WT and KO mice (Table 1). After ischemia, there was no significant difference between the two groups in several parameters such as time to no beating, time to contracture, and left ventricular end-diastolic pressure (Fig. 2). After reperfusion, however, hearts of KO mice started to beat earlier than those of WT mice (Fig. 2). At 120 min after reperfusion, contractile function (left ventricular developed pressure) of KO mice hearts was significantly better (51.7 ± 12.7% of pre-ischemic value) than that of WT mice hearts (26.3 ± 6.9%, $p < 0.05$) (Fig. 3).

Myocardial infarction after ischemia/reperfusion

After ischemia/reperfusion, there was much viable myocardium in KO hearts than WT hearts (red lesion in Fig. 4A). The infarct size was significantly smaller in KO hearts (32 ± 9%) than in WT hearts (68 ± 10%, $p < 0.05$) (white lesion in Figs. 4A and B).

Table 1
Hemodynamic parameters of NCX KO mice

	WT ($n = 6$)	NCX KO ($n = 7$)
HR(bpm)	356 ± 40	378 ± 77
LVP (mmHg)	142.8 ± 40	146.3 ± 34.5
EDP (mmHg)	4.4 ± 1.5	4.3 ± 1.3
dP/dt (mmHg/s)	7368 ± 630	7845 ± 2582
−dP/dt (mmHg/s)	5204 ± 782	5539 ± 1157
Time to no beating (min)	2.2 ± 0.9	2.2 ± 1.6
Time to contracture (min)	6.2 ± 1.7	6.3 ± 2.0
EDP at 25 min (mmHg)	67.3 ± 9.2	63.8 ± 10.8

HR, heart rate; LVP, left ventricular pressure; EDP, LV end-diastolic pressure; dP/dt and −dP/dt, positive and negative first derivatives for maximal rates of LV pressure development.

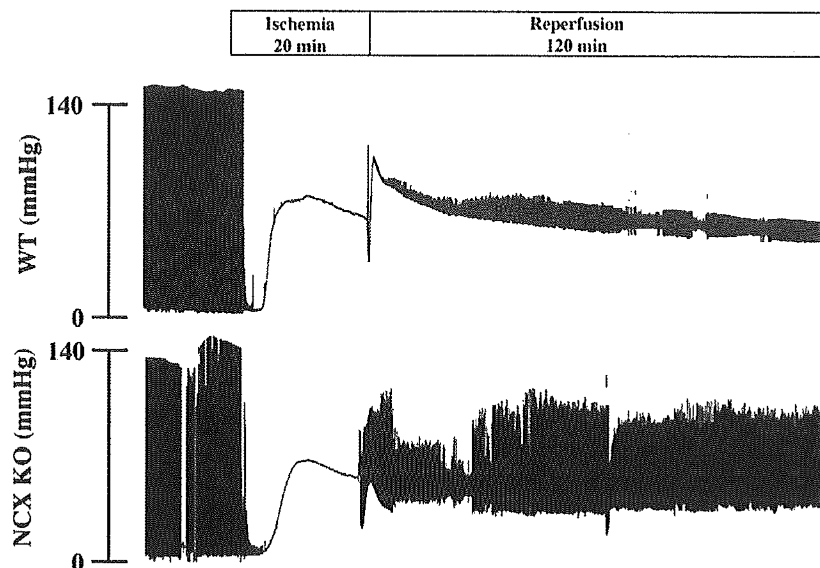

Fig. 2. Ex vivo studies. Changes in LVP during ischemia/reperfusion. Representative LVP records of WT and NCX KO mice hearts are shown. Note that KO mice hearts started to contract earlier than WT mice hearts after reperfusion.

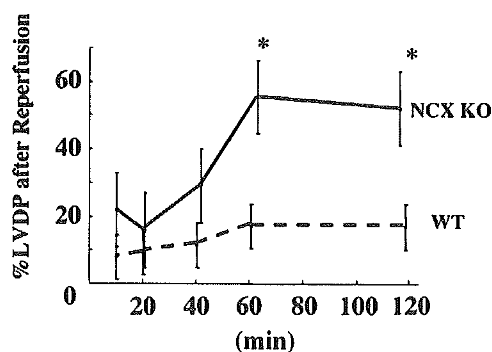

Fig. 3. LVDP of hearts of NCX KO mice ($n = 7$) and WT mice ($n = 6$) hearts after reperfusion. Values are expressed as means ± SEM. *$p < 0.05$ vs. WT mice.

Discussion

Myocardial cell injury is induced by a combination of mechanical and chemical stresses during ischemia [14]. Reoxygenation after extended periods of ischemia rapidly induces hypercontracture of cardiomyocytes [15] and aggravates the pre-existing injury [16]. The hypercontracture represents a major cause of acute lethal cell injury in the reperfused myocardium [17,18]. It has been hypothesized that an increase in intracellular Ca^{2+} levels of cardiomyocytes through NCX induces the hypercontracture state after reperfusion but not during ischemia by the mechanism described below [5]. During myocardial ischemia, anaerobic metabolism induces acidosis both inside and outside of cardiomyocytes. The Na^+–H^+ exchanger does not operate at this moment because of no difference in H^+ concentration across the plasma membrane of cardiomyocytes. Reperfusion

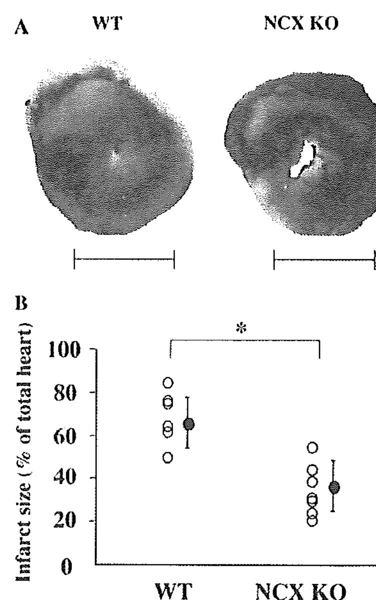

Fig. 4. (A) Representative TTC staining photographs of WT and NCX KO mice hearts after ischemia/reperfusion are shown. Infarcted area is expressed as white lesion and viable myocardium is expressed as red lesion. Bar = 2 mm. (B) Myocardial infarct size is expressed as percentage for total heart of WT mice ($n = 6$) and NCX KO mice ($n = 7$). Values are expressed as means ± SEM. *$p < 0.05$ vs. WT mice.

restores extracellular acidosis, leading to a disparity in H^+ concentration between inside and outside of cardiomyocytes. The increase in intracellular H^+ concentration activates the Na^+–H^+ exchanger, and the elevated intracellular Na^+ concentration triggers a rise in intracellular Ca^{2+} by the reverse mode of NCX [5]. The excessive Ca^{2+} overload induces the catastrophic hypercontracture of cardiomyocytes. In fact, it has been reported that reduction of Ca^{2+} concentration protects cardiomyocytes against hypercontracture evoked by reoxygenation [19]. In contrast, overexpression of NCX increased ischemia/reperfusion injury in mice [20]. Pharmacological inhibition of reverse mode of NCX protected reperfusion injury in cardiomyocytes [19]. These results suggest that NCX is critically involved in the myocardial ischemia/reperfusion injury, however, NCX inhibitors have been recently reported to be not specific to NCX [6]. Two putative NCX inhibitors, KB-R7943 and SEA0400, depressed the Ca^{2+} transients even in cardiomyocytes of NCX null mice [7]. Although these NCX inhibitors have been reported to suppress the reverse mode but not the forward mode of NCX, the administration of high dose of these inhibitors increased infarct size possibly by inhibition of forward mode of NCX [21]. We here demonstrated an important role of NCX in myocardial ischemia/reperfusion injury by using NCX KO mice. The reverse mode of NCX current in KO mice was decreased to a half of WT mice. Loss of function of NCX is assumed to result in alleviation of Ca^{2+} overload, hypercontracture, and cell death after reperfusion. Our present study clearly indicates that the inhibition of NCX contributes to cardioprotection against myocardial ischemia/reperfusion injury and suggests that specific inhibitors of reverse mode of NCX may be useful to prevent the myocardial ischemia/reperfusion injury.

Acknowledgments

We thank to Y. Reien for the current density analysis and R. Kobayashi, E. Fujita, M. Watanabe, M. Iida, and A. Ohkubo for technical assistance. This work was supported in part by grants from Japanese Ministry of Education, Science, Sports and Culture, and Japan Health Sciences Foundation.

References

[1] D. Schulze, P. Kofuji, R. Hadley, M.S. Kirby, R.S. Kieval, A. Doering, E. Niggli, W.J. Lederer, Sodium/calcium exchanger in heart muscle: molecular biology, cellular function, and its special role in excitation–contraction coupling, Cardiovasc. Res. 27 (1993) 1726–1734.

[2] J.H. Bridge, J.R. Smolley, K.W. Spitzer, The relationship between charge movements associated with I_{Ca} and I_{Na-Ca} in cardiac myocytes, Science 248 (1990) 376–378.

[3] A.G. Kleber, Resting membrane potential, extracellular potassium activity, and intracellular sodium activity during acute global ischemia in isolated perfused guinea pig hearts, Circ. Res. 52 (1983) 442–450.

[4] J.G. Pilitsis, F.G. Diaz, M.H. O'Regan, J.W. Phillis, Inhibition of Na^+/Ca^{2+} exchange by KB-R7943, a novel selective antagonist, attenuates phosphoethanolamine and free fatty acid efflux in rat cerebral cortex during ischemia–reperfusion injury, Brain Res. 916 (2001) 192–198.

[5] B.N. Eigel, R.W. Hadley, Antisense inhibition of Na^+/Ca^{2+} exchange during anoxia/reoxygenation in ventricular myocytes, Am. J. Physiol. Heart Circ. Physiol. 281 (2001) H2184–H2190.

[6] H. Reuter, S.A. Henderson, T. Han, T. Matsuda, A. Baba, R.S. Ross, J.I. Goldhaber, K.D. Philipson, Knockout mice for pharmacological screening: testing the specificity of Na^+/Ca^{2+} exchange inhibitors, Circ. Res. 91 (2002) 90–92.

[7] K. Wakimoto, K. Kobayashi, O.M. Kuro, A. Yao, T. Iwamoto, N. Yanaka, S. Kita, A. Nishida, S. Azuma, Y. Toyoda, K. Omori, H. Imahie, T. Oka, S. Kudoh, O. Kohmoto, Y. Yazaki, M. Shigekawa, Y. Imai, Y. Nabeshima, I. Komuro, Targeted disruption of Na^+/Ca^{2+} exchanger gene leads to cardiomyocyte apoptosis and defects in heartbeat, J. Biol. Chem. 275 (2000) 36991–36998.

[8] M. Suzuki, R.A. Li, T. Miki, H. Uemura, N. Sakamoto, Y. Ohmoto-Sekine, M. Tamagawa, T. Ogura, S. Seino, E. Marban, H. Nakaya, Functional roles of cardiac and vascular ATP-sensitive potassium channels clarified by Kir 6.2-knockout mice, Circ. Res. 88 (2001) 570–577.

[9] Y. Watanabe, J. Kimura, Inhibitory effect of amiodarone on Na^+/Ca^{2+} exchange current in guinea-pig cardiac myocytes, Br. J. Pharmacol. 131 (2000) 80–84.

[10] J. Kimura, S. Miyamae, A. Noma, Identification of sodium–calcium exchange current in single ventricular cells of guinea-pig, J. Physiol. 384 (1987) 199–222.

[11] Y. Zou, I. Komuro, T. Yamazaki, S. Kudoh, H. Uozumi, T. Kadowaki, Y. Yazaki, Both Gs and Gi proteins are critically involved in isoproterenol-induced cardiomyocyte hypertrophy, J. Biol. Chem. 274 (1999) 9760–9770.

[12] M. Suzuki, N. Sasaki, T. Miki, N. Sakamoto, Y. Ohmoto-Sekine, M. Tamagawa, S. Seino, E. Marban, H. Nakaya, Role of sarcolemmal K(ATP) channels in cardioprotection against ischemia/reperfusion injury in mice, J. Clin. Invest. 109 (2002) 509–516.

[13] E. Takimoto, A. Yao, H. Toko, H. Takano, M. Shimoyama, M. Sonoda, K. Wakimoto, T. Takahashi, H. Akazawa, M. Mizukami, T. Nagai, R. Nagai, I. Komuro, Sodium calcium exchanger plays a key role in alteration of cardiac function in response to pressure overload, FASEB J. 16 (2002) 373–378.

[14] H.M. Piper, D. Garcia-Dorland, M. Ovize, A fresh look at reperfusion injury, Cardiovasc. Res. 38 (1998) 291–300.

[15] B. Siegmund, A. Koop, T. Klietz, P. Schwartz, H.M. Piper, Sarcolemmal integrity and metabolic competence of cardiomyocytes under anoxia-reoxygenation, Am. J. Physiol. 258 (1990) H285–H291.

[16] M.D. Stern, A.M. Chien, M.C. Capogrossi, D.J. Pelto, E.G. Lakatta, Direct observation of the "oxygen paradox" in single rat ventricular myocytes, Circ. Res. 56 (1985) 899–903.

[17] J.A. Barrabes, D. Garcia-Dorado, M. Ruiz-Meana, H.M. Piper, J. Solares, M.A. Gonzalez, J. Oliveras, M.P. Herrejon, J. Soler-Soler, Myocardial segment shrinkage during coronary reperfusion in situ. Relation to hypercontracture and myocardial necrosis, Pflugers Arch. 431 (1996) 519–526.

[18] C.E. Ganote, Contraction band necrosis and irreversible myocardial injury, J. Mol. Cell. Cardiol. 15 (1983) 67–73.

[19] C. Schafer, Y. Ladilov, J. Inserte, M. Schafer, S. Haffner, D. Garcia-Dorado, H.M. Piper, Role of the reverse mode of the Na^+/Ca^{2+} exchanger in reoxygenation-induced cardiomyocyte injury, Cardiovasc. Res. 51 (2001) 241–250.
[20] H.R. Cross, L. Lu, C. Steenbergen, K.D. Philipson, E. Murphy, Overexpression of the cardiac Na^+/Ca^{2+} exchanger increases susceptibility to ischemia/reperfusion injury in male, but not female, transgenic mice, Circ. Res. 83 (1998) 1215–1223.
[21] J. Inserte, D. Garcia-Dorado, M. Ruiz-Meana, F. Padilla, J. Barrabes, P. Pina, L. Agullo, H. Piper, J. Soler-Soler, Effect of inhibition of Na^+/Ca^{2+} exchanger at the time of myocardial reperfusion on hypercontracture and cell death, Cardiovasc. Res. 55 (2002) 739.

ELSEVIER

Available online at www.sciencedirect.com

SCIENCE DIRECT®

Biochemical and Biophysical Research Communications 314 (2004) 1014–1020

BBRC

www.elsevier.com/locate/ybbrc

Direct measurement of Ca^{2+} concentration in the SR of living cardiac myocytes

Hiroki Kasai,[a,1] Atsushi Yao,[a,1] Tomomi Oyama,[b] Hiroshi Hasegawa,[b] Hiroshi Akazawa,[b] Haruhiro Toko,[b] Toshio Nagai,[b] Koichiro Kinugawa,[a] Osami Kohmoto,[c] Kei Maruyama,[d] Toshiyuki Takahashi,[a] Ryozo Nagai,[a] Atsushi Miyawaki,[e] and Issei Komuro[b,*]

[a] *Department of Cardiovascular Medicine, Graduate School of Medicine, University of Tokyo, Tokyo, Japan*

[b] *Department of Cardiovascular Science and Medicine, Chiba University Graduate School of Medicine, Chiba 260-8670, Japan*

[c] *The Second Department of Medicine, Saitama Medical School, Japan*

[d] *Department of Pharmacology, Saitama Medical School, Japan*

[e] *Laboratory for Cell Function and Dynamics, Advanced Technology Development Center, Brain Science Institute, The Institute of Physical and Chemical Science (RIKEN), Japan*

Received 17 December 2003

Abstract

Although abnormal sarcoplasmic reticulum (SR) Ca^{2+} handling may cause heart failure, there has been no method to directly measure Ca^{2+} concentration in SR ($[Ca^{2+}]_{SR}$) of living cardiomyocytes. We have measured $[Ca^{2+}]_{SR}$ by expressing novel fluorescent Ca^{2+} indicators *yellow cameleon* (YC) 2.1, YC3er, and YC4er in cultured neonatal rat cardiomyocytes. The distribution of YC2.1 was uniform in the cytoplasm, while that of YC3er/YC4er, containing the signal sequence which recruits them to SR, showed reticular pattern and was co-localized with SERCA2a. The treatment with caffeine reversibly decreased the emission ratio (R) in YC3er/YC4er-expressing myocytes, and the treatment with ryanodine and thapsigargin decreased R irreversibly. During the contraction–relaxation cycle, R was changed periodically in the YC2.1- and YC3er-expressing myocytes, but its direction of the change was opposite. These results suggest that YC3er/YC4er were specifically localized and functioned in SR as a $[Ca^{2+}]_{SR}$ indicator. This technique would be useful to understand the function of SR in failing myocardium.
© 2004 Elsevier Inc. All rights reserved.

Keywords: Sarcoplasmic reticulum; Fluorescent Ca^{2+} indicators; Yellow cameleon; Real-time monitoring; Cardiomyocyte; Caffeine; Thapsigargin; SERCA; Heart failure

Ca^{2+} is the primary regulator for the contraction–relaxation cycle in cardiac muscle, and the sarcoplasmic reticulum (SR) is a key organelle for physiological Ca^{2+} regulation in mammalian cardiomyocyte [1]. The accumulation of a small amount of Ca^{2+} in the diad junctions through the voltage dependent L-type Ca^{2+} channels induces a release of large amount of Ca^{2+} from SR through ryanodine receptors by the Ca^{2+}-induced Ca^{2+} release (CICR) mechanism, leading to myocardial contraction.

During relaxation, cytosolic Ca^{2+} concentration ($[Ca^{2+}]_{cyt}$) is decreased by sequestration into SR by the SR Ca^{2+}-ATPase (SERCA) or efflux from the cytosol by Na^{+}/Ca^{2+} exchanger (NCX) [2]. Dysfunction of the Ca^{2+} handling proteins of SR has recently been focused as one of the critical factors to cause heart failure [3–6]. Therefore, direct and precise measurement of the intra-SR Ca^{2+} concentration ($[Ca^{2+}]_{SR}$) in living cardiomyocyte is a prerequisite for understanding a molecular link between SR functions and heart failure. Since the kinetics of $[Ca^{2+}]_{SR}$ have been obtained from calculations based on many complicated assumptions such as Ca^{2+} buffering capacity of SR, SR volume, ionic strength, and performance of SERCA, and ryanodine receptors

* Corresponding author. Fax: +81-43-226-2557.
E-mail address: komuro-tky@umin.ac.jp (I. Komuro).
[1] These authors equally contributed to this work.

0006-291X/$ - see front matter © 2004 Elsevier Inc. All rights reserved.
doi:10.1016/j.bbrc.2003.12.189

[7–10], $[Ca^{2+}]_{SR}$ transient during every contraction–relaxation cycle has been only speculated. Recently, we have developed Ca^{2+} sensitive proteins yellow cameleons (YC) [11]. Among YC, YC3er, and 4er have the signal sequence which recruits them into the endoplasmic reticulum (ER), and reflect Ca^{2+} concentration in ER ($[Ca^{2+}]_{ER}$) in response to various stimulations in living non-muscle cells. So we have examined the real-time change of $[Ca^{2+}]_{SR}$ in living ventricular myocytes using YC3er and 4er.

Methods

This investigation conformed to the Guide for the Care and Use of Laboratory Animals (Washington, DC: Natl. Acad. Press, 1996).

Cell culture. Primary cultures of cardiac myocytes were prepared from ventricles of 1-day-old neonatal Wistar rats [12]. In brief, cells enzymatically dissociated from the ventricles were plated at a field density of 1×10^5 cells/cm^2 on 25 × 50 mm of collagen-coated coverslips in culture medium (Dulbecco's modified Eagle's medium with 10% fetal bovine serum). Twelve hours after seeding, the culture medium was changed to the medium with 0.5% fetal bovine serum.

Constructs of yellow cameleons. Plasmids containing YC2.1, YC3er, and YC4er were described previously [13]. YC3er and YC4er have a mutation of E104Q and E31Q, respectively, which is important for determination of the dissociation constant (K_d value). They also have the calreticulin leading sequence in the N terminus and the retention signal (KDEL) in the C terminus to introduce and detain these products in ER, respectively.

Transfection procedure of cameleon expression vectors. Twelve hours after plating the cells on coverslips, plasmid DNA of each cameleon was transfected using FuGENE6 (Roche, Basel, Switzerland). One microgram of DNA mixed with 3 μl of FuGENE6 reagent was added in the culture medium. The transfection efficiency of each experiment was ~5%, as determined by counting the number of cells which had significant emission of 530 nm-fluorescence excited by 420 ± 20 nm-light.

Staining of SR Ca^{2+}-ATPase (SERCA) 2a and actin filaments. After the transfection procedure, the cells were fixed with 4% paraformaldehyde-containing PBS and then permeated by 0.2% Triton X-contained PBS. For the immunostaining of SERCA2a, the cells were blocked with 5% fetal calf serum-contained PBS, incubated with affinity-purified monoclonal anti-SERCA2a antibodies (Affinity Bioreagents), and subsequently incubated with secondary fluorescein-conjugated anti-mouse IgG antibodies (CHEMICON, Temecula, USA). For the staining of the actin filaments, the permeated cells were stained with TRITC-labeled phalloidin (Sigma–Aldrich, St. Louis, USA).

Confocal images. Images were obtained using a confocal laser scanning microscopy system equipped with argon-laser and an acousto-optic tunable filter (Leica, Wetzlar, Germany). To obtain the fluorescence images from the cameleons and fluo-3, cells were excited at a wavelength of 488 nm and the emission light of 500–535 nm was acquired. The loading of fluo-3 was performed as described previously [14]. For the images of SERCA2a and actin filaments, cells were excited at 543 nm and then the emission light at 555–700 nm was acquired.

Measurement of $[Ca^{2+}]_{cyt}$ and $[Ca^{2+}]_{SR}$. The measurement of Ca^{2+} concentration was carried out with a modification of the method used for indo-1 [15]. In brief, cells were perfused with Hepes solution (126 mM NaCl, 4.4 mM KCl, 1.0 mM $MgCl_2$, 13 mM NaOH, 1.08 mM $CaCl_2$, 11 mM glucose, and 24 mM Hepes, adjusting pH to 7.4 at 25 °C) at a constant flow rate ($\geqslant$ 2 ml/min) in a heated chamber (24–6 °C) which was equipped on the stage of an inverted epifluorescence microscope (Nikon Diaphot). A myocyte expressing YC could be selected by the image of emission fluorescence passing through the dichroic mirror (DM455, Nikon), and non-myocytes having YCs fluorescence could be screened out because they did not contract in response to pacing stimulation. The myocyte within the field was then excited with the light from a 100 W mercury-arc lamp (Nikon) passing through a 420 ± 20 nm band pass filter (BV-2A, Nikon), and an emission fluorescence was detected simultaneously at 480 (BA, Nikon) and 530 nm (DF30, Omega) with a photomultiplier tube (PMT; model 1897 AH, Hamamatsu). The fluorescence of the optical field without YCs positive cells was measured as zero.

Data analysis. The emission signals from the YCs were digitized using a Digidata1200A analog-to-digital converter (Axon Instruments) and stored in a personal computer (Gateway). The data were analyzed with Axoscope1.0 (Axon Instruments) and Origin4.0 (Microcal) software.

Results

Expressing pattern of cameleons

YC2.1, YC3er, and YC4er were successfully expressed in cultured neonatal rat ventricular myocytes (Fig. 1). The protein of YC2.1 was localized in the cytosol in a homogeneous pattern except for the space probably occupied by intra-cellular organelles (Fig. 1A). As compared with the conventional Ca^{2+} sensitive dye fluo-3 (Fig. 1B), expression of YC2.1 was spared in the nucleus, suggesting that expression of YC2.1 is localized in the cytoplasm of cardiomyocytes. In contrast, YC3er showed fine reticular expression pattern around the nucleus and a ladder-like pattern in the peripheral region of cardiomyocytes (Fig. 1C). Immunocytochemisty using TRITC-labeled phalloidin revealed that the parallel lines of fine reticular region corresponded to the middle of actin filaments (I bands) (Figs. 1D–F), where there are diad junctions. Since these results suggest that YC3er is localized in SR, we examined the co-localization of YC3er and the SR protein SERCA2a. The expression pattern of YC3er was very similar to that of SERCA2a (Figs. 1G–I). The distribution of YC4er was also similar to that of YC3er (data not shown). Co-localization of YC3er and YC4er with SERCA2a at I bands suggests that YC3er and YC4er were located in SR membranes.

Ca^{2+} transient measured by cameleons

To evaluate the dynamics of intra-cellular Ca^{2+} transient, the emitted fluorescences of 480 and 530 nm from cameleons excited by 420 ± 20 nm-light were simultaneously recorded, and the ratio of 530- to 480 nm-intensity (R) was calculated. In the YC2.1-expressing myocyte, the end diastolic R was continuously raised by pacing (0.5 Hz) (Fig. 2a), and beat-to-beat oscillated R transient was seen during each contraction–relaxation cycle (Fig. 2a-A), which was quite similar to the signal monitored by use of conventional Ca^{2+} sensitive dyes

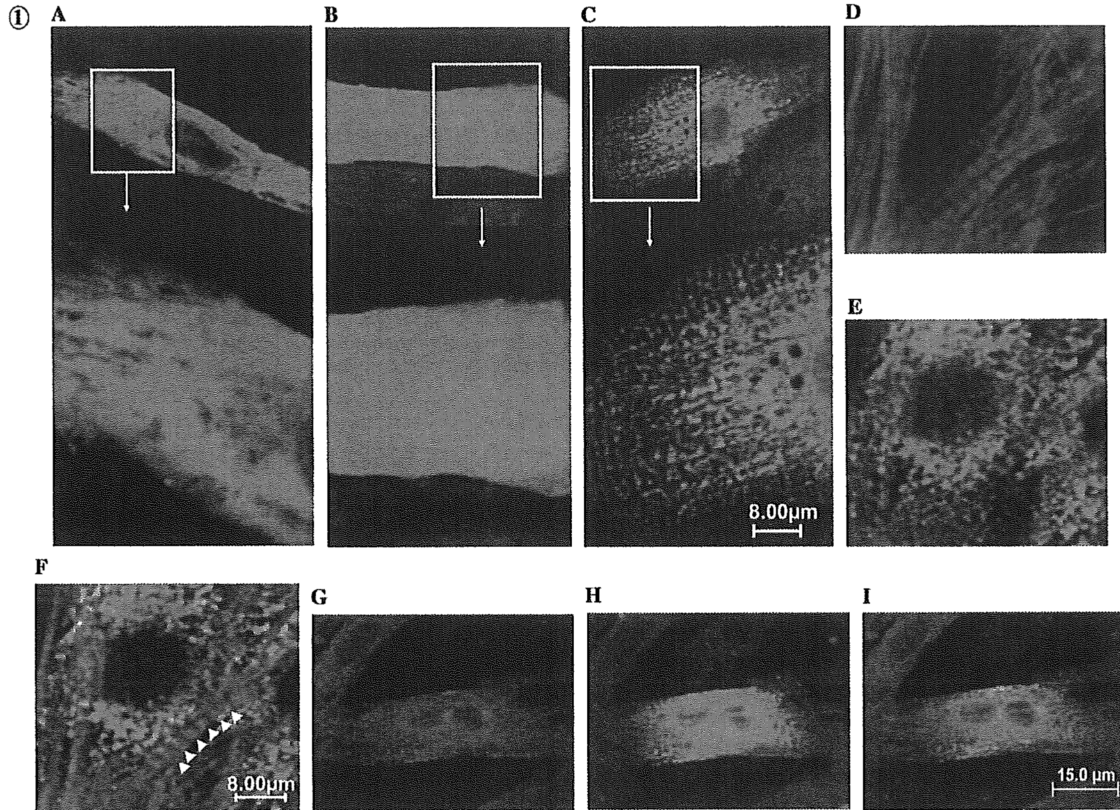
① A
B
C
D
E
8.00μm
F
8.00μm
G
H
I
15.0 μm

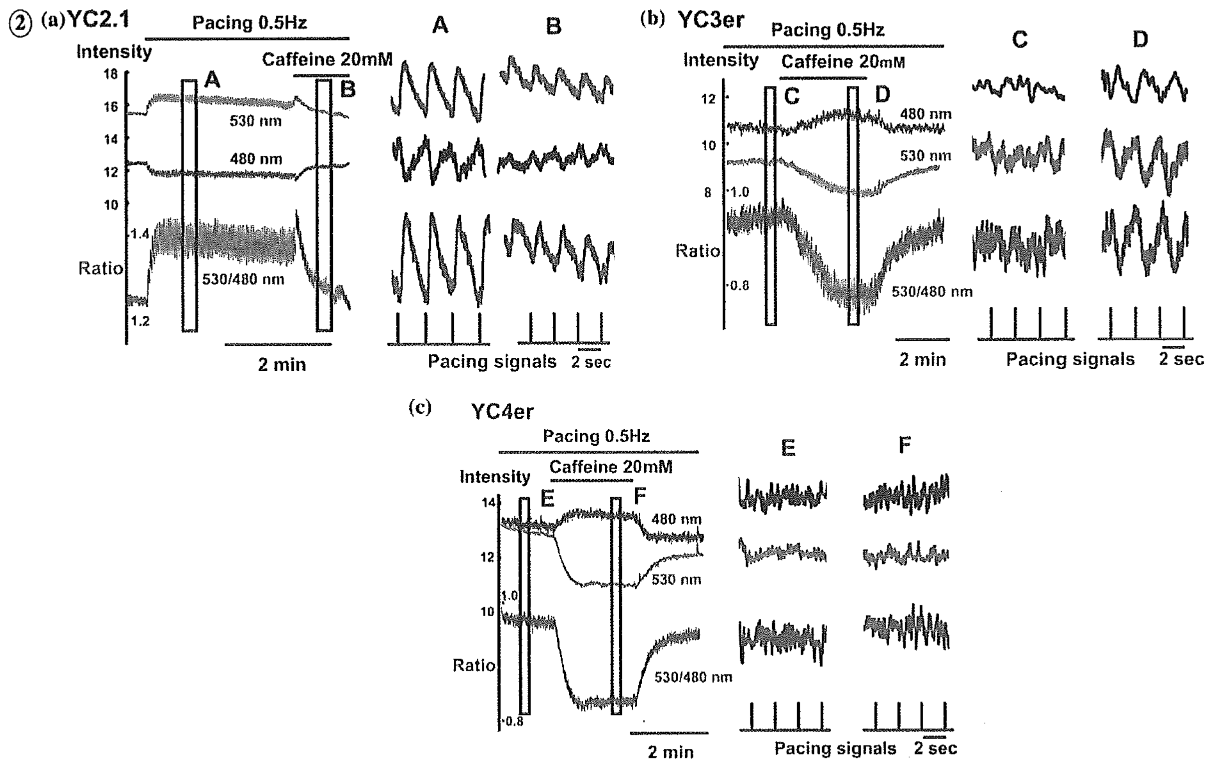
② (a)YC2.1
Pacing 0.5Hz
Intensity
Caffeine 20mM
530 nm
480 nm
Ratio
530/480 nm
2 min
A
B
Pacing signals
2 sec
(b) YC3er
Pacing 0.5Hz
Caffeine 20mM
480 nm
530 nm
530/480 nm
C
D
(c) YC4er
E
F